
©2014

KUN MEI

ALL RIGHTS RESERVED

**ASSESSMENT OF POPULATION
EXPOSURES TO AIRBORNE ALLERGENIC
POLLEN IN THE US FROM 1994 TO 2010**

by

KUN MEI

A thesis submitted to the

Graduate School-New Brunswick

Rutgers, The State University of New Jersey

in partial fulfillment of the requirements

for the degree of

Master of Science

Graduate Program in Chemical and Biochemical Engineering

written under the direction of

Panos G. Georgopoulos

and approved by

New Brunswick, New Jersey

May 2014

ABSTRACT OF THE THESIS

Assessment of Population Exposures to Airborne Allergenic Pollen in the US from 1994 To 2010

By Kun Mei

Thesis Director:

Professor Panos G. Georgopoulos

Airborne allergenic pollen is a main cause of Allergic Airway Disease (AAD), which affects 5%-30% of the population in industrialized countries. Furthermore, allergenic pollen has been reported to act synergistically with common air pollutants, such as ozone and particulate matter, to exacerbate allergy symptoms. Studies of population exposures to allergenic pollen will help to provide useful information for the scientific community to aid allergy sufferers.

In the present study, a probabilistic exposure modeling system has been developed using Monte Carlo methods to simulate exposures of the general population in the United States (US) to airborne allergenic pollen. Simulations were conducted by sampling randomly from distributions of outdoor and indoor allergenic pollen concentrations and distributions of activity data for the general US population. These activity data include time spent indoors and outdoors, inhalation rates, exposed skin area, hand-to-mouth touch frequency, etc. Distributions of airborne allergenic

pollen concentrations from representative trees, weeds and grass in nine climate regions in contiguous US were developed from observed airborne pollen counts collected at the American Academy of Allergy Asthma and Immunology (AAAAI) monitoring stations. US demographic data were used to generate the distributions of activities stratified by age and gender in the corresponding climate regions.

The mean and standard deviation of “virtual individual” daily inhalation intakes from 1994 to 2000 in the contiguous US (CONUS) were 74 ± 193 (mean \pm 1std.) pollen grains/day for ragweed (*Ambrosia*), 213 ± 687 pollen grains/day for mugwort (*Artemisia*), 146 ± 616 pollen grains/day for birch (*Betula*), 72 ± 237 pollen grains/day for grasses (*Gramineae*), and 401 ± 1312 pollen grains/day for oak (*Quercus*), during their respective pollen periods. The mean and standard deviation of daily “virtual individual” daily inhalation intakes from 2003 to 2010 in the CONUS were 162 ± 540 pollen grains/day for ragweed (*Ambrosia*), 121 ± 284 pollen grains/day for mugwort (*Artemisia*), 163 ± 780 pollen grains/day for birch (*Betula*), 114 ± 368 pollen grains/day for grasses (*Gramineae*), and 667 ± 1974 pollen grains/day for oak (*Quercus*), during their respective pollen periods.

Global sensitivity analysis of the simulations, based on Morris’ design, was used to investigate sensitivity and interaction effects of the daily intakes of allergenic pollen to the model parameters and inputs.

Exposure estimates were sensitive to parameters such as indoor ventilation rate, density of pollen, removal coefficient of pollen on the skin and efficiency of adherence to skin. The inhalation route contributes 140 times higher pollen exposure levels than the dermal contact route and 157 times higher pollen exposure levels than the unintentional ingestion route for subjects of the general population.

Acknowledgement

Foremost, I would like to express my sincere gratitude to my advisor, Prof. Panos G. Georgopoulos, for his continuous support of my master study and research, for his patience, motivation, enthusiasm, and immense knowledge. His guidance helped me through all of the research and writing of this thesis. I could not have imagined having a better advisor and mentor for my master study.

Besides my advisor, I would like to thank the rest of my thesis committee: Prof. Roth and Prof. Androulakis, for their encouragement, insightful comments, and challenging questions.

My sincere thanks also go to Yong Zhang and Linda Everett, for offering generous help and advice on this exciting project.

I thank my colleagues in the Computational Chemodynamics Laboratory: Steven Royce, Ting Cai, Zhongyuan Mi, Jocelyn Alexander and Dwaipayan Mukherjee, for the stimulating discussions, for the days working together, and for all the fun we have had in the last 8 months. Also I thank my friends at Rutgers University: Yusu Zhu, Renchang Tan, Tony Zhou, Jianli Cheng, and Suyang Wu.

Last but not least, I would like to thank my family: my parents Xiaoke Mei and Cuiling Tao, for giving birth to me in the first place and supporting me spiritually throughout my life.

Table of Contents

ABSTRACT OF THE THESIS	ii
Acknowledgement	iv
Table of Contents	v
List of figures	vii
List of Tables.....	xi
1 Background Information	1
1.1 Pollen and allergy	1
1.2 Pollen Season	2
2 Methods.....	4
2.1 Data Collection.....	4
2.1.1 Pollen Data Collection	4
2.1.2 Pollen Trend	4
2.1.3 Population Data and Exposure Factors	5
2.2 Exposure Method Selection.....	6
2.2.1 Inhalation	6
2.2.2 Dermal Exposure	9
2.2.3 Unintentional Ingestion.....	13
2.2.4 Exposure Calculation Method.....	13
2.3 Sensitivity/Uncertainty Analysis	14
3 Results and Discussion	16

3.1	Pollen Seasons	16
3.2	Pollen Concentrations.....	17
3.3	Pollen Trends	21
3.4	Exposures to Pollen	22
3.5	Sensitivity Analysis	27
4	Future Works	29
5	Conclusions.....	30
6	Figures.....	31
7	Tables	58
8	Appendix.....	75 74
9	References.....	76 75

List of figures

Figure 1. Locations of the American Academy of Allergy Asthma and Immunology (AAAAI) monitoring stations measuring airborne pollen counts in the United States	31
Figure 2. Nine climate regions in the contiguous United States (CONUS).	32
Figure 3. Spatial distribution of (a) <i>Ambrosia</i> , (b) <i>Artemisia</i> , (c) <i>Betula</i> , (d) <i>Gramineae</i> , (e) <i>Quercus</i> in the contiguous US (CONUS).....	33
Figure 4. Population by gender in nine climate regions in Contiguous United States	34
Figure 5. US population distribution of inhalation rates for males and females.	35
Figure 6. US population of distribution of surface area of human body of males and females.	36
Figure 7. Three different exposure intake routes for airborne pollen	37
Figure 8. Schematic diagram of modeling exposure to pollen in 9 climate regions...	38
Figure 9. General scheme for a sampling-based sensitivity and uncertainty analysis..	39
Figure 10. Time series of observed daily pollen concentration of <i>Ambrosia</i> at Cherry Hill, NJ (top) and Newark, NJ (bottom) monitor stations which are located in the Northeast Climate Region.....	40
Figure 11 Time series of observed daily pollen concentration of <i>Artemisia</i> in Cherry Hill, NJ (top) and Newark,NJ (Bottom) monitor stations which are located in the Northeast Climate Regions.	41

Figure 12. Time series of observed daily pollen concentration of Betula in Cherry Hill, NJ (top) and Newark, NJ (bottom) monitor stations which are located in the Northeast.	42
Figure 13. Time series of observed daily pollen concentration of Gramineae in Cherry Hill, NJ (top) and Newark, NJ (bottom) monitor stations which are located in the Northeast.	43
Figure 14. Time series of observed daily pollen concentration of Quercus in Cherry Hill, NJ (top) and Newark, NJ (bottom) monitor stations which are located in the Northeast.	44
Figure 15. Cumulative probability distributions of observed airborne daily pollen concentration for Ambrosia in the nine climate regions of contiguous US in 1994-2000 (top) and 2003-2010 (bottom).	45
Figure 16. Cumulative probability distributions of observed airborne daily pollen concentration for Artemisia in the nine climate regions of contiguous US in 1994-2000 (top) and 2003-2010 (bottom).	46
Figure 17. Cumulative probability distributions of observed airborne daily pollen concentration for Betula in the nine climate regions of contiguous US in 1994-2000 (top) and 2003-2010 (bottom)	47
Figure 18. Cumulative probability distributions of observed airborne daily pollen concentration for Gramineae in the nine climate regions of contiguous US in 1994-2000 (top) and 2003-2010 (bottom)	48
Figure 19. Cumulative probability distributions of observed airborne daily pollen concentration for Quercus in the nine climates regions of contiguous US in 1994-2000 (top) and 2003-2010 (bottom)	49

Figure 20 The heat map shows the trend of the mean daily concentrations of pollen of five species in nine climate regions of CONUS.	50
Figure 21. Simulated cumulative probability distribution of daily intake via inhalation of Ambrosia pollen in the different climate regions in 1994-2000 (top) and 2003-2010 (bottom)..	51
Figure 22. Simulated cumulative probability distribution of daily intake via inhalation of Artemisia pollen in the different climate regions in 1994-2000 (top) and 2003-2010 (bottom)..	52
Figure 23. Simulated cumulative probability distribution of daily intake via inhalation of Betula pollen in the different climate regions in 1994-2000 (top) and 2003-2010 (bottom)..	53
Figure 24. Simulated cumulative probability distribution of daily intake via inhalation of Gramineae pollen in the different climate regions in 1994-2000 (top) and 2003-2010 (bottom)..	54
Figure 25. Simulated cumulative probability distribution of daily intake via inhalation of Quercus pollen in the different climate regions in 1994-2000 (top) and 2003-2010 (bottom)..	55
Figure 26 The heat map shows the trend of the mean daily inhalation intakes of “virtual individuals” of the population of pollen of five species in nine climate regions of CONUS.....	56
Figure 27. Mean and Standard Deviation of Normalized Sensitivity Coefficient (NSC) for population exposure in Central Climate Region: (A) Inhalation, (B) Dermal, (C) Ingestion, (D) Total Exposures.	57

List of Tables

Table 1. Coordinates, elevation, main climate characteristics of the studied AAAAI pollen monitoring stations.....	58
Table 2. Parameters for calculating population exposure to pollen in nine different climate regions in CONUS. These parameters were listed either as fixed values, known distributions, or unknown empirical distributions derived from the literature (Sofiev et al., 2013).	61
Table 3. Median and mean(\pm standard deviation) of the exposure in Northeast climate region through different exposure routes (pollen grains/day) in 1994-2000 ..	64 63
Table 4. Comparisons of mean peak values between periods 1994-2000 and 2003-2010. Red values indicate that those species in those regions vary significantly over time.	65 64
Table 5. Comparisons of mean of pollen concentrations between periods 1994-2000 and 2003-2010.. Red values indicate that those species in those regions vary significantly over time.	66 65
Table 6. Median and range of the inhalation intakes in nine climate regions of contiguous US 1994-2000(pollen grains/day)	67 66
Table 7. Median and range of the inhalation intakes in nine climate regions of contiguous US in 2003-2010 (pollen grains/day)	70 69
Table 8. Mean and standard deviation of the individual inhalation intake values in 9 climate regions in 1994-2000 (pollen grains/day)	73 72
Table 9. Mean and standard deviation of the individual inhalation intakes in 9 climate regions in 2003-2010 (pollen grains/day)	74 73

1 Background Information

Airborne allergenic pollen, acting synergistically with air pollutants like ozone, will cause allergic airway disease (AAD), resulting to increased related health care costs (e.g. Lamb et al., 2006; Singh et al., 2010). It has been reported that over one third of the US population suffer from allergic symptoms and diseases at different levels, including rhinitis, hay fever, asthma, and atopic dermatitis (Bielory et al., 2012). These allergic diseases can be potentially triggered and/or aggravated by allergenic pollen, such as ragweed, birch, grass, mugwort and oak (Shea et al., 2008).

1.1 Pollen and allergy

Pollen allergies often cause hypersensitivity syndromes in the human body, including asthma, rhinitis and conjunctivitis, which can appear in the same patient simultaneously during the pollen season (Sofiev et al., 2013). The key role in the pollen allergies mechanism is the IgE (antibody immunoglobulin E), a class of antibodies in humans. The human body will overproduce IgE in response to exposure to allergenic pollen in the membranes lining the nose. The allergens then attach to the IgE on the surface of certain immune cells, which release chemicals that can cause inflammation and increase mucus in human airways. Allergic rhinitis symptoms, such as rhinorrhea, nasal obstruction, nasal itching and sneezing, may then occur (Brożek et al., 2010).

Sensitization occurs at the primary site of allergen exposure, i.e. airways, but can also occur through dermal contact. However, not everybody who is exposed via dermal contact will become sensitized and have allergic reactions (Sofiev et al., 2013).

Pollen grains, as compared to other allergens carried in outdoor as well as indoor air, have a relatively large size – with a diameter typically between 15 and 60 μm – from anemophilic plants that include trees, grasses and weeds, which produce great quantities of lightweight pollen grains during their respective pollen seasons. In this thesis, five different species are considered, specifically ragweed (*Ambrosia*), mugwort (*Artemisia*), birch (*Betula*), grasses (*Gramineae*) and oak (*Quercus*). Pollen grains are generally too large, few of them can directly penetrate into the lung (Hansen et al., 2002), most pollen grains can only adhere to the mucus covering the outside membrane of the upper respiratory tract (Behrendt & Becker, 2001).

1.2 Pollen Season

Observations and measurements, such as phenological events (i.e. flowering and withering) and pollen counts, are used to characterize the phenomenon of plant flowering. Both phenological and aerobiological data can be analyzed using methods such as regression to predict phenological phases, start and end dates of the pollen season, and the peak value of pollen. An alternative approach involves “phenological models” which can also predict the starting dates of phenological phases as well as the start, peak, and end of the pollen season. Phenological models are sometimes classified as process-based models (Chuine et al., 2000), as they are based on

mechanistic assumptions rooted in experimental results on plant physiological responses to various environmental variables. In this thesis, pollen counts are used as the key data to calculate the length and start dates of plant flowering.

2 Methods

2.1 Data Collection

2.1.1 Pollen Data Collection

Data of observed airborne pollen were retrieved from the measurements at the American Academy of Allergy Asthma and Immunology (AAAAI) monitoring stations performed during the period of 1994-2000 and 2001-2010 individually in the contiguous US (CONUS) (Zhang et al., 2013a). The geographic locations and main climate characteristics of the AAAAI pollen monitoring stations are shown in [Figure 1](#) and [Table 1](#). The reported pollen data were classified only at the level of genus. Species with the genera of Ambrosia, Artemisia, Betula, Gramineae or Quercus were not differentiated. The collected airborne pollen counts were used to generate the distributions of daily average pollen concentrations in nine climate regions of contiguous US, as shown in [Figure 2](#). The distributions of those species in the CONUS can be seen in [Figure 3](#). Dark green indicates species present and native. Light green indicates species is not rare.

2.1.2 Pollen Trend

Climate change and other phenological factors may affect pollen concentrations, and pollen concentrations may be different for each year (Zhang et al., 2013a). For the purpose of the present study and to investigate the trend of the pollen counts over time, pollen concentration data for 1994 to 2010 are divided into two parts: 1994-2000(7 years long) and 2003-2010 (8 years long).

域代码已更改

域代码已更改

域代码已更改

域代码已更改

域代码已更改

域代码已更改

带格式的：检查拼写和语法

带格式的：字体颜色：黑色

带格式的：字体颜色：黑色

带格式的：字体颜色：黑色

, since pollen data in year 2001 and year 2002 are not public accessible Two values are used to estimate the trend: mean of pollen concentration (C_{mean}) and mean of maximum pollen concentration (C_{mean_max}) per monitor station per year.

$$C_{mean} = \frac{\sum_{i=1}^n \sum_{j=1}^m \sum_{k=1}^l c_{i,j,k}}{n \times m \times l} \quad (2.1)$$

$$C_{mean_max} = \frac{\sum_{i=1}^n \sum_{j=1}^m \max_k(c_{i,j,k})}{n \times m} \quad (2.2)$$

1. i indicates year i
2. j indicates monitor station j
3. k indicates day k
4. c indicates concentration (pollen grains/m³) in a single day

2.1.3 Population Data and Exposure Factors

Population data were retrieved from the United States Census Bureau Demographic data on the general population (U.S Census Bureau, 2010). The demographic data were classified as the state-level population by age group and gender. We used ArcGIS version 10.2 (ESRI, 2013) to compile population data stratified by age and gender in nine climate regions in contiguous US (see [Figure 4](#)) and to couple them with the corresponding airborne pollen data. To perform Monte Carlo simulations, a random sample of individuals, that represent the age and gender structure of the full population, was developed for each of the climate regions. Exposure factors were obtained from USEPA's Exposure Factors Handbook (USEPA, 2010). These factors include inhalation rate ([Figure 5](#)), dermal

域代码已更改

域代码已更改

带格式的: 字体颜色: 黑色, 图案: 清除 (白色)

contact frequency, skin surface area (~~Figure 6~~Figure-6), hand surface ratio, and time spent indoors and outdoors in different age groups and within genders. The data of inhalation rates and skin surface areas, which are descriptive statistics (from 5th to 95th percentiles) were used to generate nonparametric distributions. Data of dermal contact frequency, hand surface ratio and time spent indoors and outdoors, which include means and standard deviation values, were used to generate lognormal distributions. In each age group exposure factors were used to generate exposure scenarios for each randomly sampled “virtual individual” in each of the nine climate regions in contiguous US.

These exposure factors characterize population variability at the national level. Inhalation rate distribution and other exposure factors are the same for different climate regions, although the temperature, day and night time, and other environmental factors may affect values of those factors.

2.2 Exposure Method Selection

Exposures to allergenic pollen can occur via inhalation and dermal contact (Sofiev et al., 2013), as well as unintentional ingestion (Cohen et al., 1979). ~~Figure 7~~Figure-7 illustrates the three routes of exposure.

带格式的: 检查拼写和语法

2.2.1 Inhalation

Exposure-related intakes are often quantified by multiplying the concentration of an agent and the exposure duration. “Exposure can be instantaneous when the contact between an agent and a target occurs at a single point in time and space” (USEPA, 2010). The summation of instantaneous exposures over the exposure

duration is called the time-integrated exposure. Equation 3 defines a time-integrated intake (Fogh & Andersson, 2000).

$$E = \int_{t_1}^{t_2} C \times I(t) dt \quad (2.3)$$

域代码已更改

where:

1. E is ime-integrated intake for each day (pollen grains)
2. $t_2 - t_1$ is exposure duration (one day in the current study)
3. C is mean daily exposure concentration (pollen grains/m³)
4. I is Inhalation rate (m³/day)

Time-averaged intakes are obtained by dividing the integrated intake by exposure duration.

Since human inhalation rates are different for indoors or outdoors, the “inflation” and “deflation” factors were used to represent the indoor and outdoor inhalation rate for different activity levels. Four different activity levels, which are resting and napping, light work, moderate work and heavy work, were considered to generate the inflation and deflation factors for each age group in indoor and outdoor environments.

Inhalation rate for age group i in indoor environment $I_{in,i}$ was derived using equation , Inhalation rate for age group i in outdoor environment $I_{out,i}$ was derived using equation ~~(2.5)~~(2.5), Average inhalation rate for age group i $I_{total,i}$ was derived

带格式的: 字体颜色: 黑色, 图案: 清除 (白色)

using equation ~~(2.6)~~(2.6). “Inflation” and “deflation” factors $F_{in,i}$, $F_{out,i}$ were derived using equation ~~(2.7)~~(2.7) and ~~(2.8)~~(2.8), respectively.

$$I_{in,i} = \frac{\sum_{j=1}^4 I_{i,j} \times t_{i,j} \times T_{in,j} / (T_{in,j} + T_{out,j})}{\sum_{j=1}^4 t_{i,j} \times T_{in,j} / (T_{in,j} + T_{out,j})} \quad (2.4)$$

$$I_{out,i} = \frac{\sum_{j=1}^4 I_{i,j} \times t_{i,j} \times T_{out,j} / (T_{in,j} + T_{out,j})}{\sum_{j=1}^4 t_{i,j} \times T_{out,j} / (T_{in,j} + T_{out,j})} \quad (2.5)$$

$$I_{total,i} = \frac{\sum_{j=1}^4 I_{i,j} \times t_{i,j}}{\sum_{j=1}^4 t_{i,j}} \quad (2.6)$$

$$F_{in,i} = \frac{I_{in,i}}{I_{total,i}} \quad (2.7)$$

$$F_{out,i} = \frac{I_{out,i}}{I_{total,i}} \quad (2.8)$$

1. i : indicates age group i (14 age groups from 1 month old to 64 years old)
2. j : indicates activity level j (resting, light, moderate, heavy)
3. $I_{in,i}$, $I_{out,i}$ and $I_{total,i}$ are indoor, outdoor and mean inhalation rate (m^3 /hour), respectively
4. $I_{i,j}$ is inhalation rate at activity level j and age group i (m^3 /hour)
5. $t_{i,j}$ is time spent at j activity level and i age group (hour)
6. $T_{out,j}$ $T_{in,j}$ is time spent indoors and outdoors at j activity level.(hour)
7. $F_{in,i}$, $F_{out,i}$ are inflation factor and deflation factor for inhalation rate in two different environments (indoors and outdoors)

Since only daily averages of airborne pollen concentrations are available from the AAAAI monitor network, only distribution of daily intakes can be calculated

带格式的：字体颜色：黑色，图案：清除（白色）

带格式的：字体颜色：黑色，图案：清除（白色）

带格式的：字体颜色：黑色，图案：清除（白色）

域代码已更改

域代码已更改

域代码已更改

域代码已更改

域代码已更改

through the available data. The outdoor and indoor exposures to allergenic pollen were calculated using equations ~~(2.9)~~(2.9) and ~~(2.10)~~(2.10), respectively.

带格式的: 字体颜色: 黑色

带格式的: 字体颜色: 黑色

Outdoor:

$$E_{outdoor} = \int_{t_1}^{t_2} C I_{out}(t) dt$$

(~~2.9~~2.9)

带格式的: 不检查拼写或语法, 图案: 清除 (白色)

带格式的: 不检查拼写或语法, 图案: 清除 (白色)

域代码已更改

Indoor

$$E_{indoor} = \frac{\lambda_v}{\lambda_v + \lambda_d} \int_{t_1}^{t_2} C I_{in}(t) dt$$

(~~2.10~~2.10)

域代码已更改

带格式的: 不检查拼写或语法, 图案: 清除 (白色)

带格式的: 不检查拼写或语法, 图案: 清除 (白色)

where λ_d is the indoor particle suspension coefficient (s^{-1})

批注 [mk1]: I am not quite sure about the name. Which is not explained in word in the reference.

$$\lambda_d = \frac{A_d v_d}{V}$$

(2.11)

域代码已更改

where

1. E is time-integrated exposure (pollen grains)
2. $t_2 - t_1$ is exposure duration (ED) (day)
3. C is exposure concentration as a function of time (pollen/ m^3)
4. I is inhalation factors (m^3 /day)
5. A_d is the surface area available for particle deposition (m^2)
6. V is the volume of the building (m^3)
7. v_d is the indoor deposition velocity ($m s^{-1}$)
8. λ_v is (s^{-1}) is indoor ventilation rate

2.2.2 Dermal Exposure

Dermal exposures to particulate matter have been quantitatively studied (Hu et al., 2011), but qualitative studies of dermal exposure to pollen (e.g. Björkstén et al., 1980; Sofiev et al., 2013) remain rare. We used a dry deposition model to estimate the adherence of pollen to human skin (Seinfeld & Pandis, 2012).

The dry deposition model assumes that the transport of material to the surface is governed by three resistances in series: the aerodynamic resistance r_a , the quasi-laminar layer resistance r_b , the particle settling velocity is v_s , and v_d is the deposition velocity. The fundamental equation is shown in ~~(2.11)(2.14)~~

$$v_d = v_s + \frac{1}{r_a + r_b + r_a * r_b * v_s} \quad (2.11)$$

Where the calculations of r_a , r_b , v_s are shown in equation ~~(2.11)(2.14)~~, ~~(2.11)(2.14)~~, and ~~(2.11)(2.14)~~, respectively.

$$r_a = \frac{1}{ku_*} \ln \left(\frac{z}{z_0} \right) \quad (2.11)$$

$$r_b = \frac{1}{u_* \left(S_c^{\frac{2}{3}} + 10^{-\frac{3}{S_c}} \right)} \quad (2.11)$$

$$v_s = \frac{\rho_p D_p^2 g C_c}{18\mu} \quad (2.11)$$

Where C_c is the slip correction factor, shown in equation ~~(2.11)(2.14)~~.

带格式的: 字体颜色: 黑色

带格式的: 字体颜色: 黑色, 图案: 清除 (白色)

带格式的: 字体颜色: 黑色

带格式的: 字体颜色: 黑色, 图案: 清除 (白色)

带格式的: 字体颜色: 黑色

带格式的: 不检查拼写或语法, 图案: 清除 (白色)

带格式的: 不检查拼写或语法, 图案: 清除 (白色)

带格式的: 字体颜色: 黑色

带格式的: 字体颜色: 黑色, 图案: 清除 (白色)

带格式的: 字体颜色: 黑色

带格式的: 字体颜色: 黑色, 图案: 清除 (白色)

带格式的: 字体颜色: 黑色

带格式的: 字体颜色: 黑色, 图案: 清除 (白色)

带格式的: 不检查拼写或语法, 图案: 清除 (白色)

带格式的: 不检查拼写或语法, 图案: 清除 (白色)

带格式的: 字体颜色: 黑色, 图案: 清除 (白色)

$$C_c = 1 + \frac{2\lambda}{D_p} \left(1.257 + 0.4e^{\frac{0.55D_p}{\lambda}} \right) \quad (22.114)$$

带格式的: 不检查拼写或语法

带格式的: 不检查拼写或语法

Where ρ_p is the density of the pollen grain, D_p is the aerodynamic pollen grain diameter, g is the gravitational acceleration, μ is the viscosity of air, u^* is the friction velocity, z and z_0 are reference height (at the top of the constant flux layer) and initial height (at the bottom of the constant flux layer), respectively..

The calculation of Schmidt number S_c , Stokes number S_t and the molecular diffusivity D are shown in equation (2.12)(2.12), (2.13)(2.13), (2.14)(2.14), respectively. Equation (2.14)(2.14) is also called Einstein-Stokes equation.

带格式的: 字体颜色: 黑色

带格式的: 字体颜色: 黑色, 图案: 清除 (白色)

带格式的: 字体颜色: 黑色

带格式的: 字体颜色: 黑色

$$S_c = \frac{\mu}{\rho_a D} \quad (22.1242)$$

带格式的: 不检查拼写或语法, 图案: 清除 (白色)

带格式的: 不检查拼写或语法, 图案: 清除 (白色)

$$S_t = \frac{v_s u_*^2 \rho_a}{g \mu} \quad (2.13)$$

域代码已更改

域代码已更改

$$D = \frac{k_B T C_c}{3\pi \mu D_p} \quad (22.1444)$$

域代码已更改

带格式的: 不检查拼写或语法, 图案: 清除 (白色)

带格式的: 不检查拼写或语法, 图案: 清除 (白色)

Equation (2.15)(2.15) and Equation (2.16)(2.16) show the direct deposition to the skin in indoor and outdoor environments, respectively.

带格式的: 字体颜色: 黑色

带格式的: 字体颜色: 黑色

(1) outdoor

$$M_{outdoor} = S_a \times R_t \times v_d \times c$$

(22.1545)

域代码已更改

带格式的: 不检查拼写或语法, 图案: 清除 (白色)

带格式的: 不检查拼写或语法, 图案: 清除 (白色)

(2) indoor

$$M_{indoor} = \frac{S_a \times R_t \times v_d \times \lambda_v}{\lambda_v + \lambda_d} \times c \quad (2.16+6)$$

带格式的: 不检查拼写或语法, 图案: 清除 (白色)

带格式的: 不检查拼写或语法, 图案: 清除 (白色)

域代码已更改

Where

1. M_{indoor} and $M_{outdoor}$ are daily depositions of allergenic airborne pollen on the exposed skin surface in indoor and outdoor environments, respectively.
2. S_a is the skin area (m^2).
1. R_t the ratio of the skin which are exposed to pollens (head, arm, hand, leg) (dimensionless)
3. The parameters v_d ($m \ s^{-1}$) and λ_v (dimensionless) are indoor deposition velocity and indoor ventilation rate, respectively.

After the pollen deposits on the skin, some pollen may adhere to skin, and cause an allergic reaction such as irritation and redness of the skin. We use a parameter called efficiency of adherence to skin (L_r) to illustrate this effect. In addition, the airborne pollen could be removed by many activities including wind blowing, water washing or hand/object touching., We use a parameter called removal coefficient of the pollens on the skin (R_m) to illustrate this effect. The equation is shown in (2.17)(2.17).

带格式的: 字体颜色: 黑色

$$E_{derm} = M \times L_r / (1 + rm) \quad (2.17+7)$$

域代码已更改

带格式的: 不检查拼写或语法, 图案: 清除 (白色)

带格式的: 不检查拼写或语法, 图案: 清除 (白色)

Where

2. E_{derm} is the dermal exposure

3. M the total mass of the pollen on the skin surface ($M_{indoor} + M_{outdoor}$) (pollen grains/m²)
4. R_m is the removal coefficient of the pollens on the skin (dimensionless)
5. L_r is the efficiency of adherence to skin (dimensionless).

2.2.3 Unintentional Ingestion

Another possible route is unintentional ingestion (Chivato et al., 1996; Cohen et al., 1979). Some individuals, especially children, may use hands loaded with pollen to touch the mouth, and this may cause unintentional ingestion of pollen grains. This effect may in general be neglected when we consider exposures of adults. The equation (2.18) shows this relationship.

$$E_{ingest} = \frac{M}{S_a} \cdot \frac{R_h}{1 + R_h} \quad (2.18)$$

Where

1. E_{ingest} is the ingestion exposure, the mass of the pollen intake through ingestion
2. M the total mass of the pollen on the skin surface ($M_{indoor} + M_{outdoor}$) (pollen grains/m²)
3. S_a is the total surface of human skin (m²)
4. R_h the ratio of the hands in the total skin area (dimensionless)

带格式的: 字体颜色: 黑色

域代码已更改

带格式的: 不检查拼写或语法, 图案: 清除 (白色)

带格式的: 不检查拼写或语法, 图案: 清除 (白色)

-
5. Fr is hand-to-mouth contact frequency (times/hour)
-

2.2.4 Exposure Calculation Method

A Monte Carlo simulation method was used to generate the exposure estimates. The activity data of 100,000 “virtual individuals” were compiled based on corresponding exposure factor distributions and demographic data for each climate region ([Figure 8](#)~~Figure 8~~). For example, the estimates for a “virtual” 75 year old man were generated by calculating the exposure factors for ages 71-80, male group. Then the observed data for airborne pollen counts were combined with the activity data using a Monte Carlo method, by randomly selecting values from each dataset. 100,000 exposure values were generated for each climate region. The process is schematically illustrated in [Figure 8](#)~~Figure 8~~.

2.3 Sensitivity/Uncertainty Analysis

Sensitivity analysis of a system involves the quantitative assessment of the effects of changes in its inputs to changes in its outputs. Uncertainty analysis involves attributing the uncertainty in the output of a system to sources of uncertainty in its inputs ([Figure 9](#)~~Figure 9~~).

带格式的: 检查拼写和语法

The mean daily mass intake of pollen grains was selected as a metric for testing the system’s sensitivity to multiple inputs and parameters. Global sensitivity analysis was performed based on Morris’ Design (Saltelli et al., 2000a; Saltelli et al., 2000b). Morris’ design characterized the effect of a parameter or input by computing multiple estimates of local sensitivities at random points of the parameter space. As per Zhang et al. (2013b), “The mean of these randomized local sensitivities indicates

the overall influence of a given parameter on the output metric, while the corresponding standard deviation indicates the effects of interactions and nonlinearity.”

In the present study, each of the 18 parameters involved in formulating the pollen exposure model (~~Table 2~~Table 2) was sampled 3,600 times according to the Morris method (from 200 trajectories, each with 18 steps) in the parameter space. Each of the parameters in the simulation was perturbed from 50% to 150% from its “base” value while keeping other parameters unchanged. For values in distributions, if the new value after the perturbation fell out the corresponding range of the distribution, it was folded back into the range by taking the maximum or minimum value in the range.

The mean daily intake for sensitivity analyses was generated using 100,000 “virtual individuals” in each climate regions during the flowering season. Equation 25 was used to calculate Normalized Sensitivity Coefficients (NSCs) at a local point (~~Figure 9~~Figure 9).

$$NSC_{i,j} = \frac{\frac{\Delta r_{ij}}{r_{ij}}}{\frac{\Delta p}{p}} \quad (22.1818)$$

In this equation, the $NSC_{i,j}$ is the NSC for exposure route i (inhalation, ingestion, dermal) in different climate regions j . The p is the input parameter value, and r is the corresponding daily mean output of the exposure effect. The Δr and Δp are the corresponding perturbation of the parameter values and perturbation of the output, respectively. The global NSC of a certain parameter, NSC_g , is defined as

带格式的: 字体: (中文) 宋体, 字体颜色: 黑色

带格式的: 字体: (中文) 宋体, 字体颜色: 黑色

带格式的: 不检查拼写或语法, 图案: 清除 (白色)

带格式的: 不检查拼写或语法, 图案: 清除 (白色)

the mean of the corresponding local sensitivities. The overall absolute mean $|\overline{NSC_g}|$ for each route is obtained by averaging the absolute NSC_g values for the corresponding route and region. Similarly, the overall absolute mean standard deviations $\overline{STD_g}$ are averages over each exposure route.

3 Results and Discussion

3.1 Pollen Seasons

For Newark and Cherry Hill considered in the present study, comparison of mean pollen indices between the periods of 1994–2000 and 2001–2010 showed that the five selected species (Ambrosia, Artemisia, Betula, Gramineae and Quercus) were observed to start flowering 2-15 days in average earlier during the period of 2003-2010 than in the period of 1994-2000. For different monitor stations located in other climate regions, the pollen periods for the same species are usually different among years, however, the lengths of are roughly the same.

~~Figure 10~~ ~~Figure 10~~ to ~~Figure 14~~ ~~Figure 14~~ present time series of observed daily concentrations of Ambrosia, Artemisia, Betula Gramineae and Quercus grass pollen from 1994 to 2000 and 2003 to 2010 at the Rutgers Newark (formerly UMDNJ Newark) and Cherry Hill monitoring stations in New Jersey, USA. The start date of pollen emissions for different species varies. The pollen season ranges from early March to late October, and the peak values most often appear around the middle of the pollen season.

The observed pollen season start dates varied for the five species in the United States. The following results are derived from the Newark and Cherry Hill stations as examples. The average start date was found to be 25th July for Ambrosia, for which pollen season is July to October, averaging 138 days (~~Figure 10~~ ~~Figure 10~~); 11th August for Artemisia, for which pollen season is August to October, averaging 95

带格式的：字体：(中文)+中文正文(宋体)，字体颜色：黑色，图案：清除(白色)

带格式的：字体：(中文)+中文正文(宋体)，字体颜色：黑色，图案：清除(白色)

带格式的：字体颜色：黑色，图案：清除(白色)

days (~~Figure 11~~~~Figure 11~~); 29th March for Betula, for which pollen season is March to June, averaging 112 days (~~Figure 12~~~~Figure 12~~); 28th April for Gramineae, for which pollen season is April to July, averaging 125 days (~~Figure 13~~~~Figure 13~~); and 22nd March for Quercus, for which pollen season is March to June, averaging 114 days (~~Figure 14~~~~Figure 14~~). The observations indicated that responses of different species to climate change were variable for the different climate regions. Data were analyzed for the periods from March to September, which cover the pollen seasons for all the species listed above. For some species (Betula, Gramineae and Quercus) the pollen data retrieved from monitor station located in Cherry Hill, NJ are not public available, so only data retrieved from monitor station located in Newark, NJ.

带格式的: 字体颜色: 黑色, 图案: 清除 (白色)

带格式的: 字体颜色: 黑色, 图案: 清除 (白色)

带格式的: 字体颜色: 黑色, 图案: 清除 (白色)

带格式的: 字体颜色: 黑色, 图案: 清除 (白色)

3.2 Pollen Concentrations

~~Figure 15~~~~Figure 15~~ to ~~Figure 19~~~~Figure 19~~ summarize the cumulative probabilities of pollen concentrations in the nine different climate regions of in contiguous US in periods of 1994-2000 and 2001-2010. In the period of 1994-2000, the peak values of pollen grains were 1794 pollen grains/m³ for Ambrosia, 853 pollen grains/m³ for Artemisia, 1346 pollen grains/m³ for Betula, 1320 pollen grains/m³ for Gramineae and 1027 pollen grains/m³ for Quercus, respectively. In the period of 2001-2010, the peak values of pollen grains were 948 pollen grains/m³ for Ambrosia, 1242 pollen grains/m³ for Artemisia, 1827 pollen grains/m³ for Betula, 1278 pollen grains/m³ for Gramineae and 1423 pollen grains/m³ for Quercus, respectively. Different climate regions show different pollen concentrations.

Figure 15~~Figure 15~~ shows the cumulative probabilities of pollen concentrations of Ambrosia in the nine different climate regions of in contiguous US in periods of 1994-2000 and 2001-2010. In the period 1994-2000, figure shows that the Southwest Region has the highest average pollen concentrations, in which the median pollen concentration is 55 pollen grains/m³. The West Region has the lowest average pollen concentrations, in which the median pollen concentration is 7 pollen grains/m³. Since the sizes of original data of pollen concentration of Ambrosia are very small in those nine climate regions in CONUS, the lines are quite zigzag. In the period 2003-2010, the highest pollen concentrations are found in Southwest Region, in which the median pollen concentration is 35 pollen grains/m³. the lowest average pollen concentrations are found in Central Region and EastNorthCentral Region, in which the median pollen concentration is 3 pollen grains/m³.

Figure 16~~Figure 16~~ shows the cumulative probabilities of pollen concentrations of Artemisia in the nine different climate regions of in contiguous US in periods of 1994-2000 and 2001-2010. In the period 1994-2000, the pollen concentration profiles are quite similar. The EastNorthCentral Region has the highest average pollen concentrations, in which the median pollen concentration is 28 pollen grains/m³. The Northwest Region has the lowest average pollen concentrations, in which the median pollen concentration is 9 pollen grains/m³. In the period 2003-2010, the highest pollen concentrations are found in Northeast Region, in which the median pollen concentration is 25 pollen grains/m³, the lowest average pollen concentrations are found in South Region, in which the median pollen concentration is 1 pollen grains/m³.

Figure 17~~Figure 17~~ shows the cumulative probabilities of pollen concentrations of Betula in the nine different climate regions of in contiguous US in periods of 1994-2000 and 2001-2010. In the period 1994-2000, The WestNorthCentral Region has the highest average pollen concentrations, in which the median pollen concentration is 67 pollen grains/m³. The West Region has the lowest average pollen concentrations, in which the median pollen concentration is 4 pollen grains/m³. Since the sizes of original data of pollen concentration of Betula are small in those nine climate regions in CONUS, the lines are quite zigzag. In the period 2003-2010, the highest pollen concentrations are found in South Region, in which the median pollen concentration is 53 pollen grains/m³, the lowest average pollen concentrations are found in Southwest Region and Northwest Region, in which the median pollen concentration is 3 pollen grains/m³.

Figure 18~~Figure 18~~ shows the cumulative probabilities of pollen concentrations of Gramineae in the nine different climate regions of in contiguous US in periods of 1994-2000 and 2001-2010. In the period of 1994-2000, the Northwest Region has the highest average pollen concentrations, in which the median pollen concentration is 17 pollen grains/m³. The Southwest Region has the lowest average pollen concentrations, in which the median pollen concentration is 4 pollen grains/m³. In the period of 2003-2010, the highest pollen concentrations are found in South Region, in which the median pollen concentration is 18 pollen grains/m³, the lowest average pollen concentrations are found in Southeast Region and Northwest Region, in which the median pollen concentration is 3 pollen grains/m³.

Figure 19~~Figure 19~~ shows the cumulative probabilities of pollen concentrations of Quercus in the nine different climate regions of in contiguous US in

periods of 1994-2000 and 2001-2010. In the period 1994-2000, the WestNorthCentral Region has the highest average pollen concentrations, in which the median pollen concentration is 45 pollen grains/m³. The Northwest Region has the lowest average pollen concentrations, in which the median pollen concentration is 8 pollen grains/m³. In the period 2003-2010, the highest pollen concentrations are found in South Region, in which the median pollen concentration is 89 pollen grains/m³, the lowest average pollen concentrations are found in Southwest Region and Northwest Region, in which the median pollen concentration is 5 pollen grains/m³.

In the Northeast, Central and East North Central climate regions, the mean concentrations of *Betula* and *Quercus* are higher than those in other climate regions. In the West, South and Southwest climate regions, *Ambrosia* and *Artemisia* show the higher (?) concentrations.

Surface loading was calculated based on a small particle transport model, dry deposition model, and Einstein-stokes equation. Time spent indoors and outdoors by individuals in the population would affect the human exposure scenario significantly (Fogh & Andersson, 2000). The indoor ventilation rate (λ_v) is the key parameter to describe the air exchange rate of the indoor scenario. High value of λ_v means more convection of the indoor and outdoor air, thus the concentration of pollen indoors would be closer to the concentration outdoors. Exposure data for 5 different species in the Northeast Climate Region of 1994-2000 were used to study exposures through 3 different routes (Table 3Table 3). Inhalation was found to be the dominant route compared with ingestion and dermal contact. The exposure from inhalation is about 140 times higher than the other two routes which are based on skin contact (Table 3Table 3).

The outdoor concentration of airborne pollen is normally 10-15 times higher than indoor concentrations based on the calculations on indoor ventilation rate (listed in [Table 2](#)) for airborne pollen.

3.3 Pollen Trends

The data are divided into two periods to investigate the trend of pollen concentrations over time. [Table 4](#) shows mean peak values of daily airborne pollen concentrations in periods 1994-2000 and 2003-2010 for nine different climate regions of contiguous US; [Table 5](#) shows the comparison of mean daily airborne pollen concentrations between two periods for nine climate regions of contiguous US. The red values indicate that the species in those regions vary significantly over time (using t-test). Those five species are all found varying significantly in Northeast Region. Artemisia, Betula and Gramineae are found varying significantly in West Region. Figure 20 is the heat map that shows trend of the mean daily concentrations of pollen of five species in nine climate regions of CONUS. The values shown in heat map are the standardized logarithmic values. Larger values are redder, indicating great increasing of daily concentrations in the second year period (2003-2010). Smaller values are greener, indicating great decreasing of daily concentrations in the second year period (2003-2010). Blue box shows that there is no data in that region for that species in period 1994-2000.

The mean daily pollen concentration of *Quercus* increased significantly almost all the nine climate region except Westnorthcentral Region. The Northeast and Northwest suffer the most distinct increasing which have the value 0.55 and 0.54. The Gramineae show a similar situation, but the concentration in West Region drops significantly, while the concentration in South Region increased which has the value

带格式的: 字体颜色: 黑色, 图案: 清除 (白色)

带格式的: 字体颜色: 黑色, 图案: 清除 (白色)

0.9(5.6 times higher).The pollen concentration of Betula increased in Central Northeast central and Southeast, in other regions, the pollen concentration of Betula decreased. For Artemisia, the pollen concentrations slightly increased ,comparing to other species, only in Northwest and Southwest. For Ambrosia, the pollen concentration increased dramatically in South and West region with values 0.71(3.14 times higher)) and 0.65 (2.79 times higher).

3.4 Exposures to Pollen

Since the inhalation is the dominant route of exposures in the three routes. we consider pollen intakes through inhalation route in this chapter. ~~Figure 21~~Figure 24 to ~~Figure 25~~Figure 25 show the simulated cumulative probability of individual daily inhalation intakes to pollen via the inhalation route for periods of 1994-2000 and 2003-2010. The median and range of the daily inhalation intakes of Ambrosia, Artemisia, Betula, Gramineae and Quercus are shown in ~~Table 6~~Table 6 and ~~Table 7~~Table 7 for periods of 1994-2000 and 2003-2010, respectively. The descriptive statistics of the daily inhalation intakes (mean and standard deviation) of Ambrosia, Artemisia, Betula, Gramineae, and Quercus are shown in ~~Table 8~~Table 8 and ~~Table 9~~Table 9 for 1994-2000 and 2003-2010, respectively.

~~Figure 21~~Figure 24 shows the simulated cumulative probability distribution of daily individual intake via inhalation of Ambrosia pollen in the nine climate regions in CONUS in 1994-2000 (top) and 2003-2010 (bottom). In the period 1994-2000, figure shows that the Southwest Region has the highest average daily individual intakes via

带格式的：字体：(中文) 黑体，字体颜色：黑色，图案：清除 (白色)

带格式的：字体：(中文) 黑体，字体颜色：黑色，图案：清除 (白色)

带格式的：字体：(中文) 黑体，图案：清除 (白色)

带格式的：字体：(中文) 黑体，图案：清除 (白色)

带格式的：字体：(中文) 黑体，图案：清除 (白色)

带格式的：字体：(中文) 黑体，图案：清除 (白色)

inhalation, in which the median of daily individual intakes via inhalation is 68 pollen grains/day. The West Region has the lowest average daily individual intakes via inhalation, in which the median of daily individual intakes via inhalation is 14 pollen grains/day. In the period 2003-2010, the highest daily individual intakes via inhalation are found in Northwest Region, in which the median of daily individual intakes via inhalation is 17 pollen grains/day. the lowest average daily individual intakes via inhalation are found in EastNorthCentral Region, in which the median of daily individual intakes via inhalation is 7 pollen grains/day.

Figure 22 shows the simulated cumulative probability distribution of daily individual intake via inhalation of Artemisia pollen in the nine climate regions in CONUS in 1994-2000 (top) and 2003-2010 (bottom). In the period 1994-2000, figure shows that the EastNorthCentral Region has the highest average daily individual intakes via inhalation, in which the median of daily individual intakes via inhalation is 40 pollen grains/day. The West Region has the lowest average daily individual intakes via inhalation, in which the median of daily individual intakes via inhalation is 15 pollen grains/day. In the period 2003-2010, the highest daily individual intakes via inhalation are found in EastNorthCentral Region, in which the median of daily individual intakes via inhalation is 17 pollen grains/day. the lowest average daily individual intakes via inhalation are found in Southwest Region, in which the median of daily individual intakes via inhalation is 3 pollen grains/day.

Figure 23 shows the simulated cumulative probability distribution of daily individual intake via inhalation of Betula pollen in the nine climate regions in CONUS in 1994-2000 (top) and 2003-2010 (bottom). In the period 1994-2000, figure shows that the WestNorthCentral Region has the highest average daily individual

intakes via inhalation, in which the median of daily individual intakes via inhalation is 149 pollen grains/day. The West Region has the lowest average daily individual intakes via inhalation, in which the median of daily individual intakes via inhalation is 9 pollen grains/day. In the period 2003-2010, the highest daily individual intakes via inhalation are found in South Region, in which the median of daily individual intakes via inhalation is 109 pollen grains/day. the lowest average daily individual intakes via inhalation are found in Southwest Region, in which the median of daily individual intakes via inhalation is 8 pollen grains/day.

Figure 24 shows the simulated cumulative probability distribution of daily individual intake via inhalation of Gramineae pollen in the nine climate regions in CONUS in 1994-2000 (top) and 2003-2010 (bottom), figure shows that the Northwest Region has the highest average daily individual intakes via inhalation, in which the median of daily individual intakes via inhalation is 25 pollen grains/day. The Central and EastNorthCentral Region have the lowest average daily individual intakes via inhalation, in which the median of daily individual intakes via inhalation is 11 pollen grains/day. In the period 2003-2010, the highest pollen of daily individual intakes via inhalation are found in South Region, in which the median of daily individual intakes via inhalation is 33 pollen grains/day. the lowest average daily individual intakes via inhalation are found in Southeast Region and EastNorthCentral Region, in which the median of daily individual intakes via inhalation is 10 pollen grains/day.

Figure 25 shows the simulated cumulative probability distribution of daily individual intake via inhalation of Quercus pollen in the nine climate regions in CONUS in 1994-2000 (top) and 2003-2010 (bottom). In the period 1994-2000, figure

shows that the Southeast Region has the highest average daily individual intakes via inhalation, in which the median of daily individual intakes via inhalation is 129 pollen grains/day. The Northwest Region has the lowest average pollen concentrations, in which the median pollen concentration is 21 pollen grains/day. In the period 2003-2010, the highest daily individual intakes via inhalation are found in South Region, in which the median of daily individual intakes via inhalation is 292 pollen grains/day. the lowest average daily individual intakes via inhalation are found in Southwest Region, in which the median of daily individual intakes via inhalation is 13 pollen grains/day.

In the period of 1994-2000 daily mean inhalation intakes of *Betula* pollen are relatively low comparing to other species in the same region, from 100 pollen grains/day in the Central Region to 206 pollen grains/day in the Northeast Region. The daily inhalation intakes of *Ambrosia* are slightly higher, from 86 pollen grains/day in the Northwest Region to 664 pollen grains/day in the East North Central Region. The daily inhalation intakes to *Artemisia* are the lowest, from 30 pollen grains/day in the Southeast Region to 146 pollen grains/day in the Southwest Region. The daily inhalation intakes to *Gramineae* are generally low, ranging from 31 pollen grains/day in the Southwest Region to 196 pollen grains/day in the West North Central Region. For *Quercus*, the daily inhalation intakes range widely, from 61 pollen grains/day in the Northeast to 801 pollen grains/day in the West Region. In general, 2003-2010 national-wide daily mean inhalation intakes were higher than those of 1994-2000, with one exception being *Ambrosia*, which had lower nation-wide average inhalation intakes.

~~Figure 26~~Figure 26 shows the trend of the mean daily inhalation intakes of “virtual individuals” of the population of pollen of five species in nine climate regions of CONUS. The values shown in heat map are the standardized logarithmic values. Larger values are redder, indicating great increasing of daily concentrations in the second year period (2003-2010). Smaller values are greener, indicating great decreasing of daily concentrations in the second year period (2003-2010). Blue box shows that there is no data in that region for that species in period 1994-2000.

带格式的: 检查拼写和语法

The heat map of the trend of mean individual daily inhalation intakes of five species in nine climate regions of CONUS is quite similar to the heat map of the trend of mean daily pollen concentration of five species in nine climate regions of CONUS. The mean individual daily inhalation intakes of Quercus pollen increased significantly almost all climate regions except WestNorthCentral Region. The other seven climate Regions (no data in southwest) all suffer great increasing of mean individual daily inhalation intakes of Quercus pollen, having values ranging from 0.5(the mean individual daily intakes in 2003 -2010 being 2.23 times higher than the 1994-2003 year) to 0.74(3.42 times higher). Gramineae show a similar situation with inhalation intakes increasing in Central, EastNorthCentral, Northeast, Northwest, South and Southwest Regions. Inhalation intakes in South Region show a dramatically increasing with the mean individual daily intakes in 2003 -2010 being 6.32 times higher than the 1994-2003 year .The mean individual inhalation intakes of pollen of Betula increased in Central ,Northeast, and Southeast Regions, while in the same time the West and WestNorthCentral Regions show a negative trend. In other regions, mean individual inhalation intakes of pollen of Betula nearly remain the same. For Artemisia, mean individual inhalation intakes decreased in Northeast, Southeast and West Regions, but the Southwest shows a positive trend. For Ambrosia, the mean

individual inhalation intakes are increasing in south and west regions. In Southeast, Southwest and WestNorthCentral Regions, the trend is negative.

In general, populations are suffering more inhalation intakes of Quercus and Gramineae Pollen in COUNS. However, population in Westnorthcentral region are suffering less inhalation intakes of almost all the airborne pollen of five species(no data of Artemisia)

3.5 Sensitivity Analysis

Global sensitivity, based on Morris' design (Saltelli et al., 2000b), of the simulated exposures to 18 different parameters are illustrated in [Figure 27](#) for the Central Climate Region. Overall, the global NSC of all parameters varied between -0.3 and 0.35, indicating the robustness of this modeling approach. Dermal contact and ingestion exposures are shown to be more sensitive to parameter perturbations, with absolute average global NSC of these 18 parameters, $\overline{NSC_g}$, being 0.1634 and 0.1312, respectively. Sensitivity parameters for the dermal contact route include: indoor ventilation rate (λ_v), density of pollen (P_p), removal coefficient on the skin (R_m), and friction velocity (u^*). Sensitivity parameters for the unintentional ingestion route include: density of pollen (P_p), indoor ventilation rate (λ_v), dermal loading rate (L_r), removal coefficient on the skin (R_m). Inhalation exposure is less sensitive to modeling parameters. Total exposures have nearly the same sensitivity to the 18 parameters as the inhalation exposure. This is due to the fact that exposure from inhalation is much higher than the other two routes which are based on skin contact.

High interaction and nonlinearity effects among parameters were found in dermal contact and ingestion routes for pollen exposures. Average interaction effects \overline{STD} were 0.2288 and 0.1943, in dermal contact and ingestion routes, respectively. Parameters with high interaction and nonlinearity effects included removal coefficient on the skin (R_m), female inhalation rate (Ih_f), for dermal contact routes. Parameters with high interaction and nonlinearity effects included removal coefficient on the skin (R_m) for dermal contact routes.

Uncertainties in sensitive and interactive input parameters would result in large deviations of model predictions. Parameters derived from large population studies (USEPA, 2010), such as distribution of inhalation rate (Ih_f , Ih_m) and hand surface ratio (S_r), should bear lower uncertainties. Distribution of hand to mouth touch frequency (F_r) is derived from small population size, which should bear larger uncertainties. High uncertainties are expected for these sensitive parameters: λ_v , $\overline{NSC_g} = -0.2349$; P_p , $\overline{NSC_g} = 0.3246$; R_m , $\overline{NSC_g} = 0.2334$; L_r , $\overline{NSC_g} = 0.2722$; and interactive parameters : R_m , $\overline{STD_g} = 0.3344$; L_r , $\overline{STD_g} = 0.2723$; λ_v , $\overline{STD_g} = 0.1683$.

The dermal loading rate coefficients and removal coefficient on the skin depend on surface characteristics (dry or wet), temperatures, and physical transport effects. The indoor ventilation rate depends on temperatures and aerodynamic effects. Data on these dependencies are extremely limited for pollen deposition and ventilation. The values of R_m and L_r used in the current study were derived from the literature (Cohen et al., 1979; Hu et al., 2011; Zhang et al., 2013b). The values of λ_v used in the current study were derived from (Lu & Howarth, 1996). Widely different pollen dermal contact effect due to hand touch have been reported in the literature

(Behrendt & Becker, 2001; Brożek et al., 2010). Further investigations to reduce the uncertainties in L_r and Rm , are important and crucial for accurate assessments of population exposures to pollen in the United States.

4 Future Works

批注 [k2]: This is my adding about future works.

Population data in the same year (2010 population data from US census bureau (U.S Census Bureau, 2010)) were coupled with pollen data in different years in the present study. It was not accurate since the population composition (age and gender) in each climate region of contiguous US changes through years. We will use population data of the corresponding year to couple with the pollen data in the future work.

Exposure factors such as inhalation rates and time spent indoor may not only vary among different age groups and gender, but also among different climate region (spatial variation). In the future study, we may use these data retrieved from different locations (namely south and north) to estimate the spatial distribution of these data. Thus we could generate a more accurate model to estimate the human activity in different regions of contiguous US.

Wind speed and precipitation sometimes have significantly effects on transport of airborne pollen grains, thus they would affect human exposure to airborne pollen grains. High wind speed would cause the dispersal of airborne pollen grains becomes large (Damialis et al., 2005). While precipitation would decrease the dispersal speed of pollen grains and change the surface properties of airborne pollen grain.

In the meantime, pollen grains of different specs are not identical. The sizes and morphological features can be of great differences(ERDTMAN, 1986), thus they would affect the deposited velocity in the micro-environment along the human skin surface.

5 Conclusions

- A US population exposure model was developed incorporating pollen network measurements and human activity and demographic data. Daily pollen concentration data for nine different climate regions of contiguous US were compiled from available time series data of the AAAAI network.
- Exposures to five different allergenic pollen species in nine climate regions of contiguous US have been estimated through the presented model. In general, populations in the Southwest Region experience the lowest average pollen intakes (99 pollen grains/day) while populations in the South Region experience the highest average pollen intakes (682 pollen grains/day), taking into account an average of all 5 species of interest.
- The inhalation route contributes 140 times higher pollen exposure levels than the dermal contact route and 157 times higher pollen

批注 [mk3]:

exposure levels than the unintentional ingestion route for subjects of the general population

- In addition, sensitivity analyses of the modeling system provide helpful information regarding the physical parameters that affect human exposures to allergenic pollen.

6 Figures

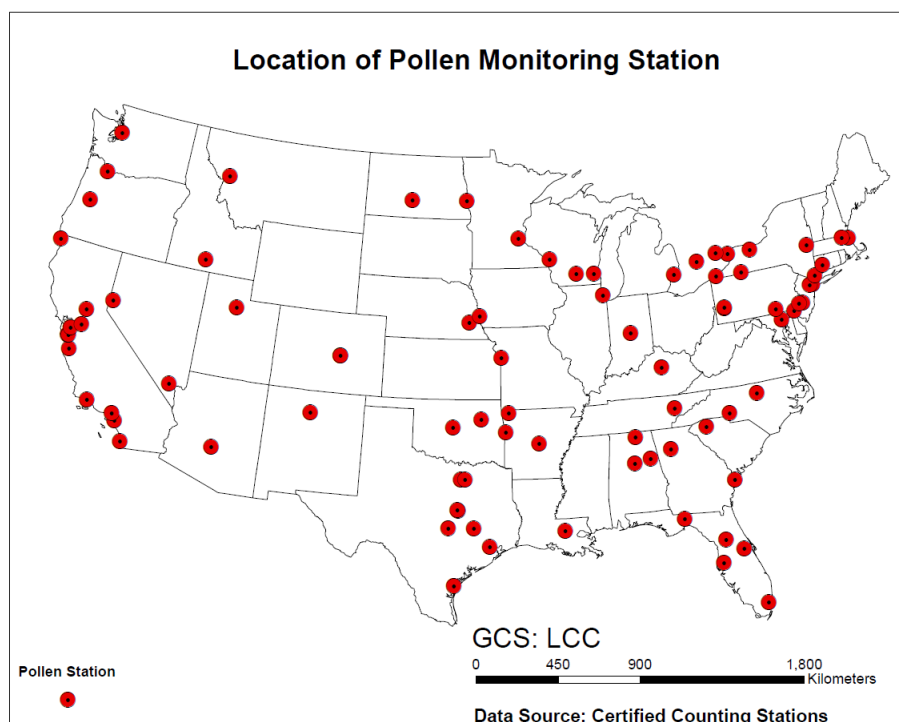


Figure 1. Locations of the American Academy of Allergy Asthma and Immunology (AAAAI) monitoring stations measuring airborne pollen counts in the United States

U.S. Climate Regions

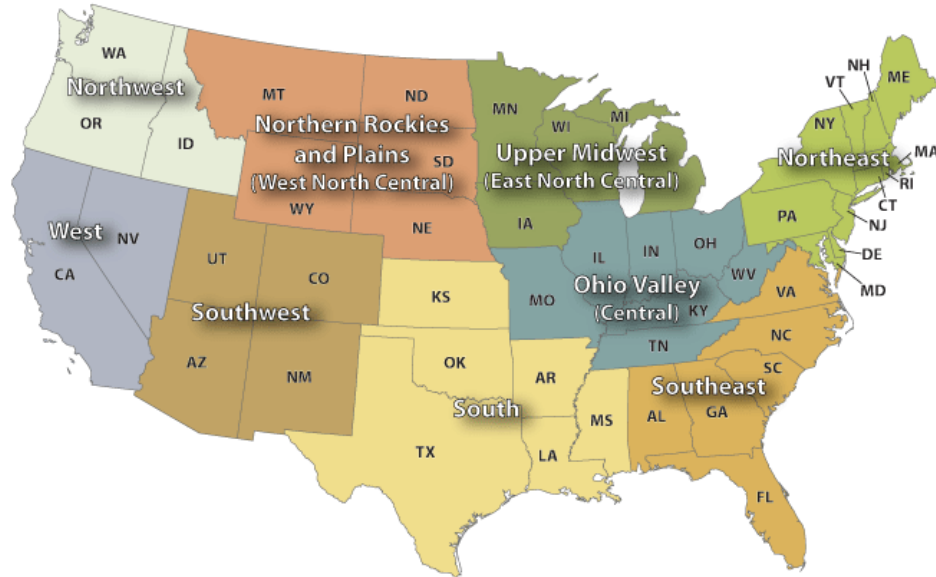


Figure 2. Nine climate regions in the contiguous United States (CONUS). Through climate analysis, National Climatic Data Center scientists have identified nine climatically consistent regions within the CONUS which are useful for putting current climate anomalies into a historical perspective (figure from Karl & Koss, 1984).

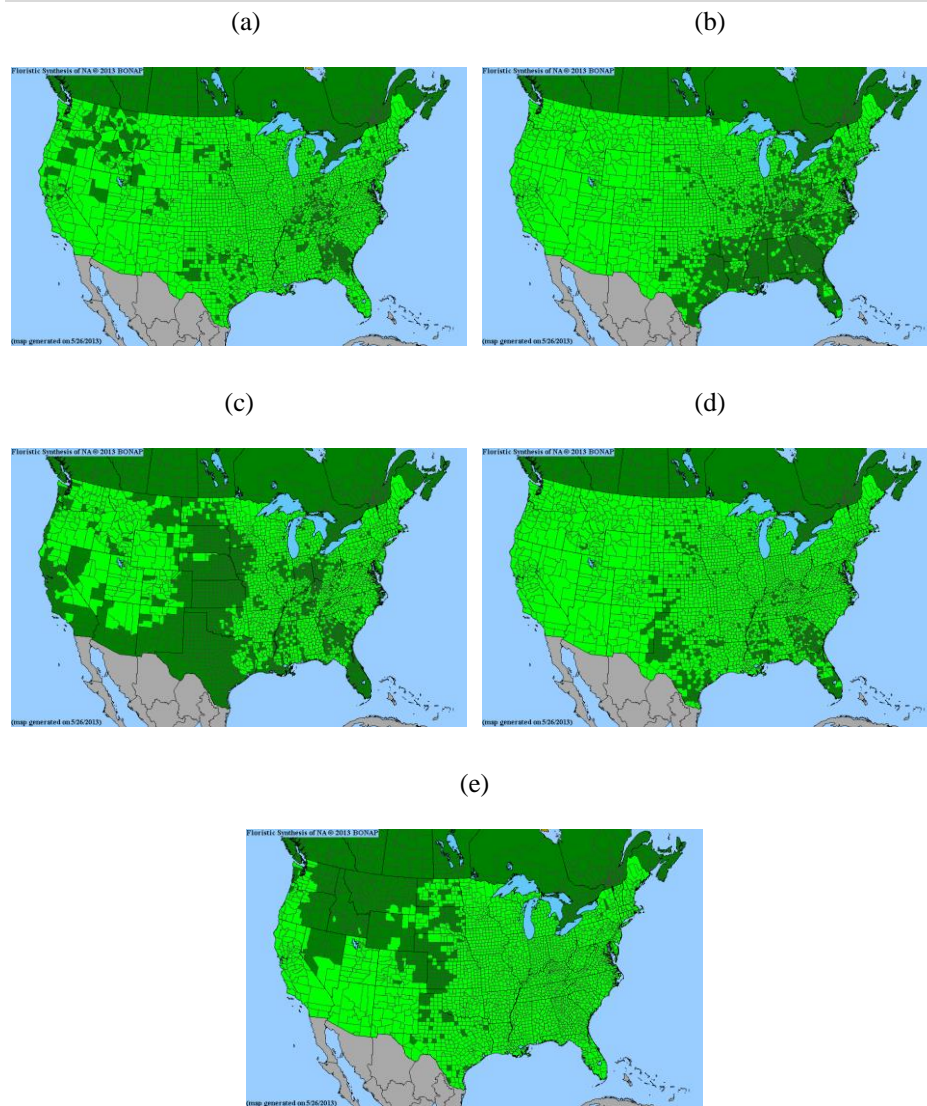


Figure 3. Spatial distribution of (a) *Ambrosia*, (b) *Artemisia*, (c) *Betula*, (d) *Gramineae*, (e) *Quercus* in the contiguous US (CONUS) (Kartesz, 2013). Dark green indicates species present and native. Light green indicates species is not rare.

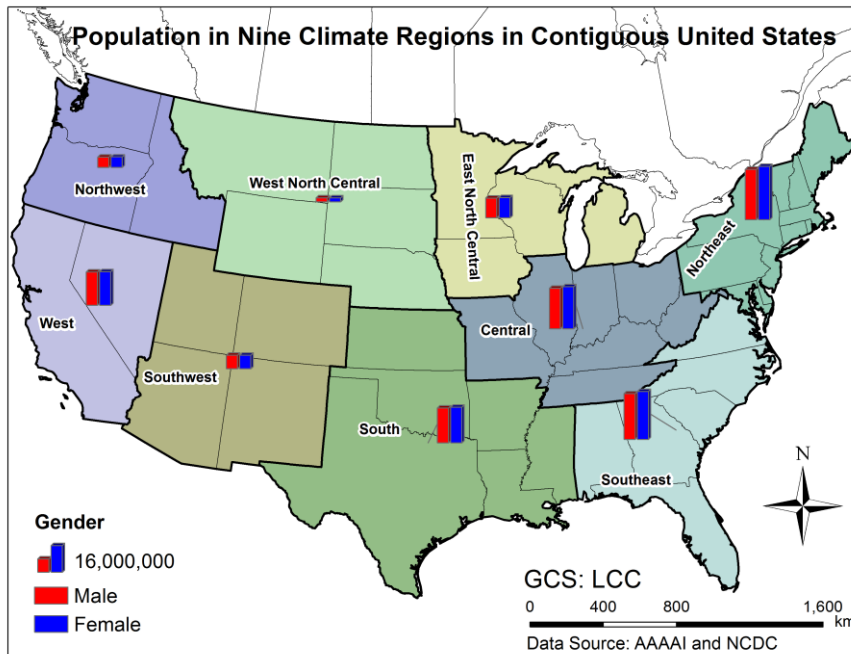


Figure 4. Population by gender in nine climate regions in Contiguous United States (CONUS)(Population data were collected in 2010,(U.S. Census Bureau, 2010))

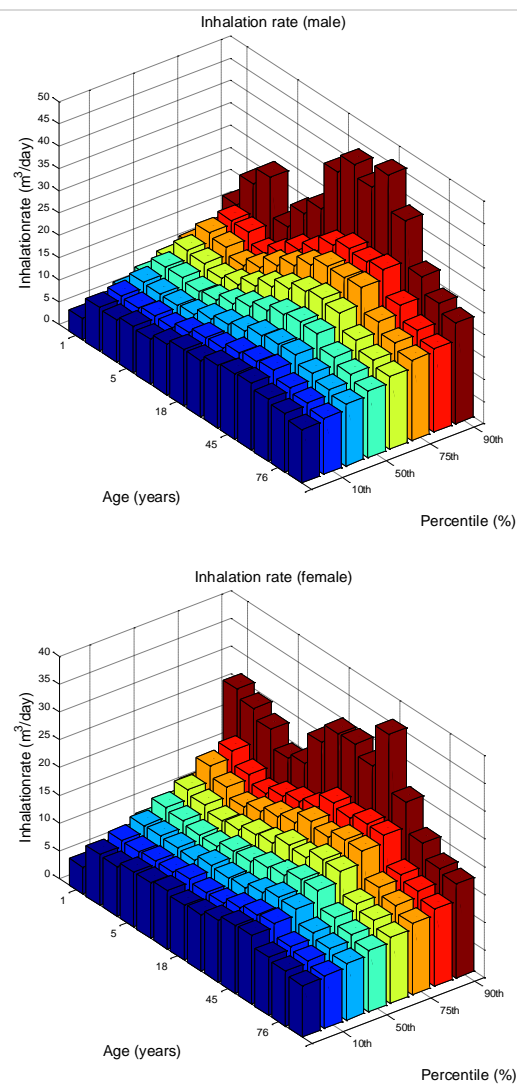


Figure 5. US population distribution of inhalation rates for males and females, respectively. The data are from EPA's Environmental Factors Handbook (USEPA, 2010). There are 14 age groups from the original data, for each gender. The age groups are 0-1 year, 1-2 years, 2-3 years, 3-6 years, 6-11 years, 11-16 years, 16-21 years, 21-31 years, 31-41 years, 41-51 years, 51-61 years, 61-71 years, and 71-81 years. The percentiles are 5th, 10th, 25th, 50th, 75th, 90th, and 95th.

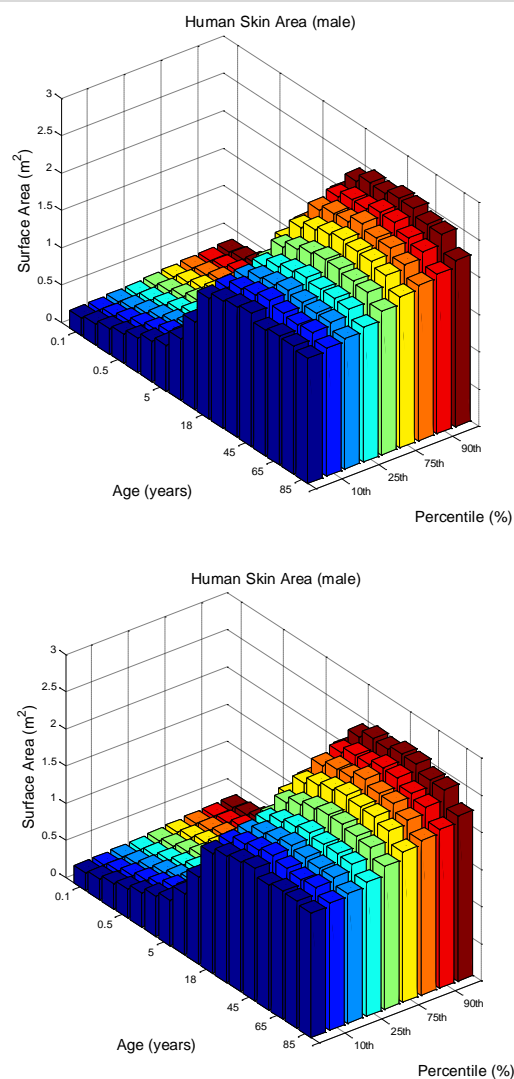


Figure 6. US population of distribution of surface area of human body of males and females, respectively. The data are from EPA's Environmental Factors Handbook (USEPA, 2010). There are 17 age groups from the original data for each gender. The age groups are less than 1month, 1-3 months, 3-6 months, 6-12 months, 1-2 years, 2-3 years, 3-6 years, 6-11 years, 11-16 years, 16-21 years, 21-31 years, 31-41 years, 41-51 years, 51-61 years, 61-71 years, and 71-81 years. 81 years and older. The percentiles are 5th, 10th, 25th, 50th, 75th, 90th, and 95th.

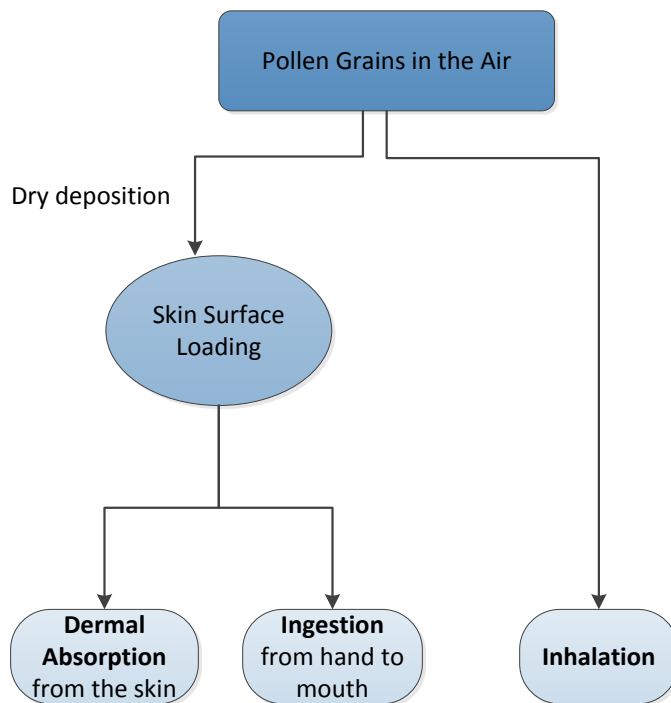


Figure 7. Three different exposure intake routes for airborne pollen

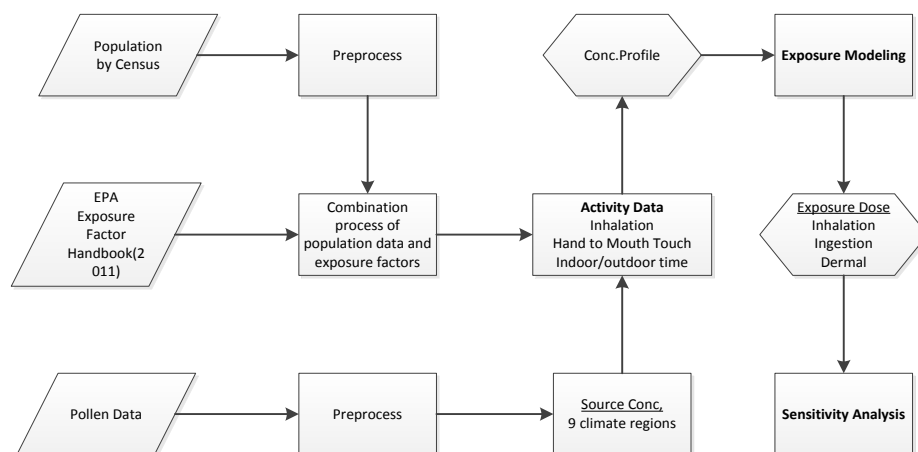


Figure 8. Schematic diagram of modeling exposure to pollen in 9 climate regions.

Concentrations and surface loading of pollen were simulated based on observed daily pollen counts from AAAAI monitoring stations. Exposures to pollen were simulated using airborne concentration profiles and activity data for different groups stratified by age and gender from the United States Census Bureau. The intake calculated from exposure modeling is then used to conduct sensitivity analysis.

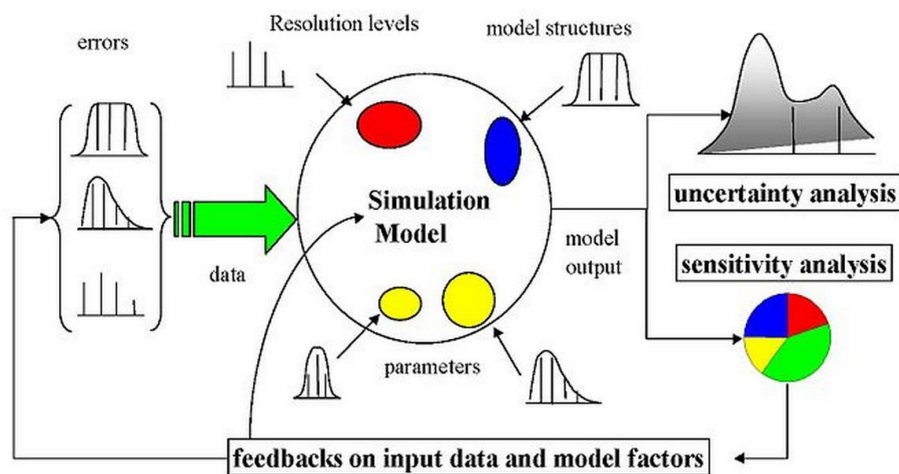


Figure 9. General scheme for a sampling-based sensitivity and uncertainty analysis.

Uncertainty can arise from different sources - errors in the data, parameter estimation procedure, and alternative model structures - they are propagated through the model for uncertainty analysis and their relative importance is quantified via sensitivity analysis (figure from Saltelli et al., 2000b).

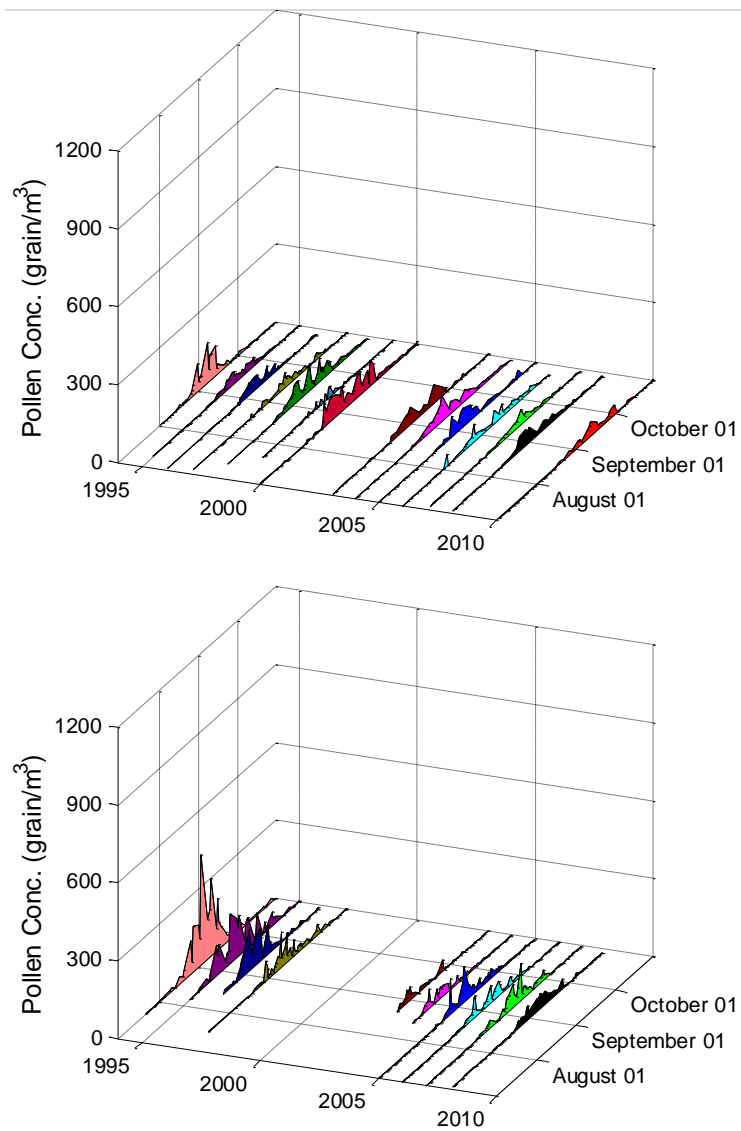


Figure 10. Time series of observed daily pollen concentration of Ambrosia at Cherry Hill, NJ (top) and Newark, NJ (bottom) monitor stations which are located in the Northeast Climate Region. The pollen data are from Dr. Leonard, Bielory.

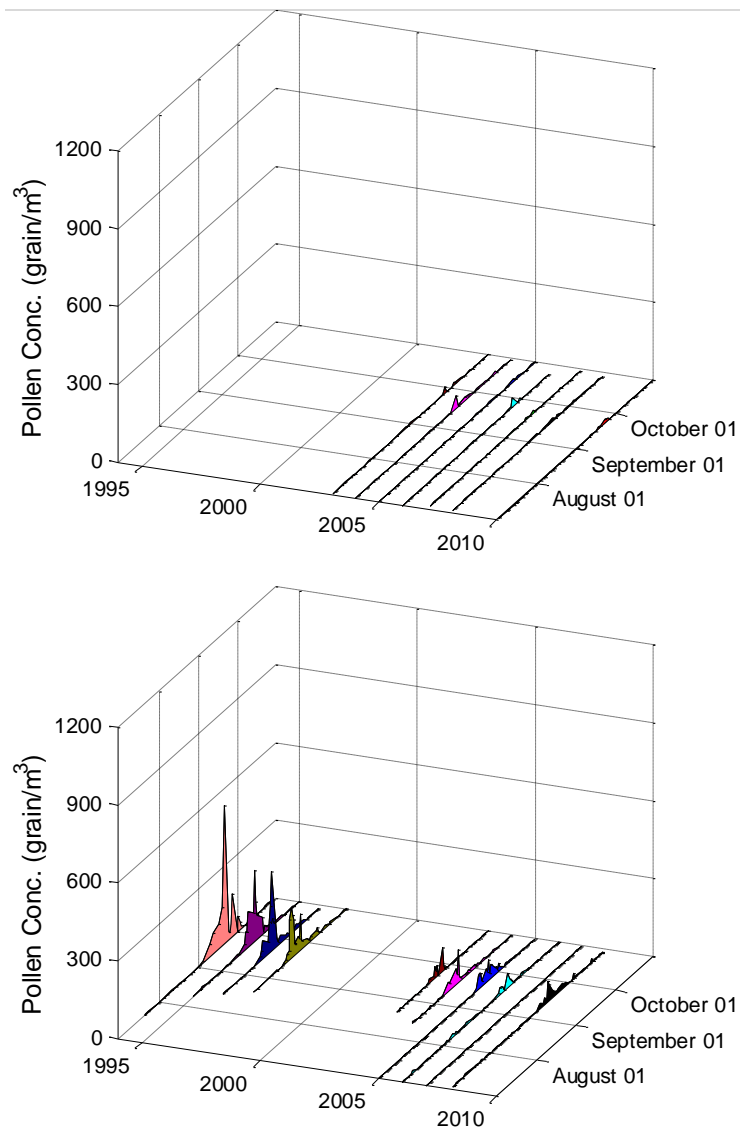


Figure 11 Time series of observed daily pollen concentration of Artemisia in Cherry Hill, NJ (top) and Newark, NJ (Bottom) monitor stations which are located in the Northeast Climate Regions. The pollen data are from Dr. Leonard, Bielory.

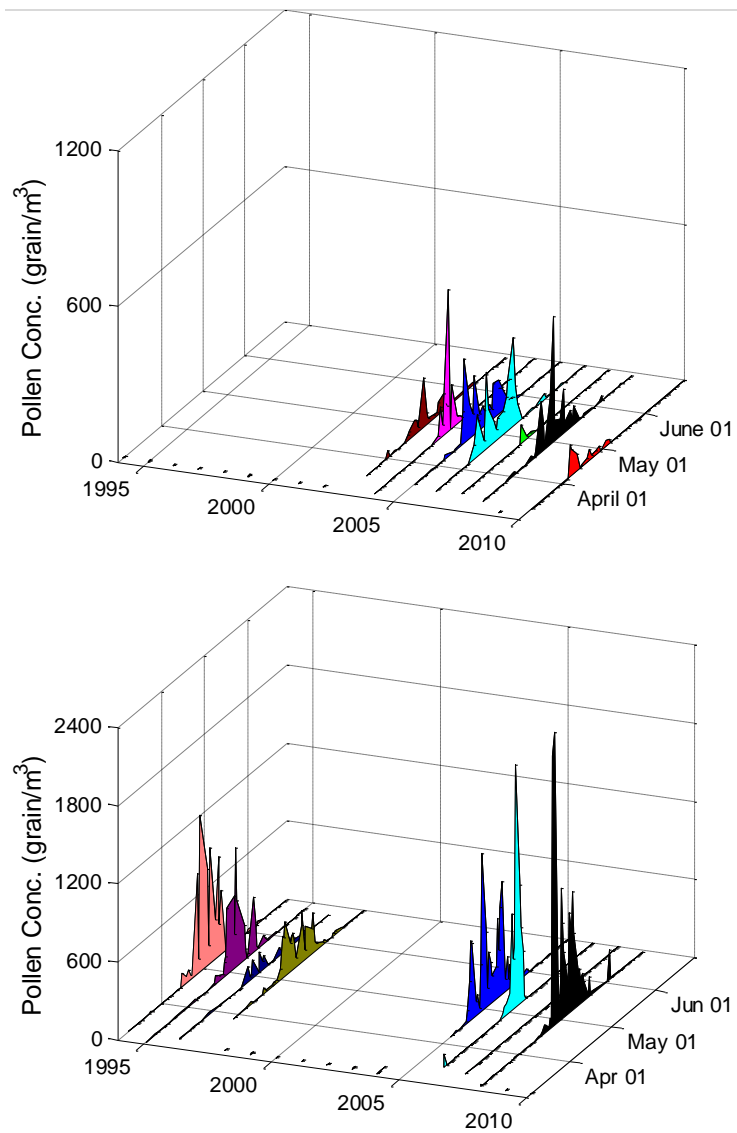


Figure 12. Time series of observed daily pollen concentration of Betula in Cherry Hill, NJ (top) and Newark, NJ (bottom) monitor stations which are located in the Northeast. The pollen data are from Dr. Leonard, Bielory.

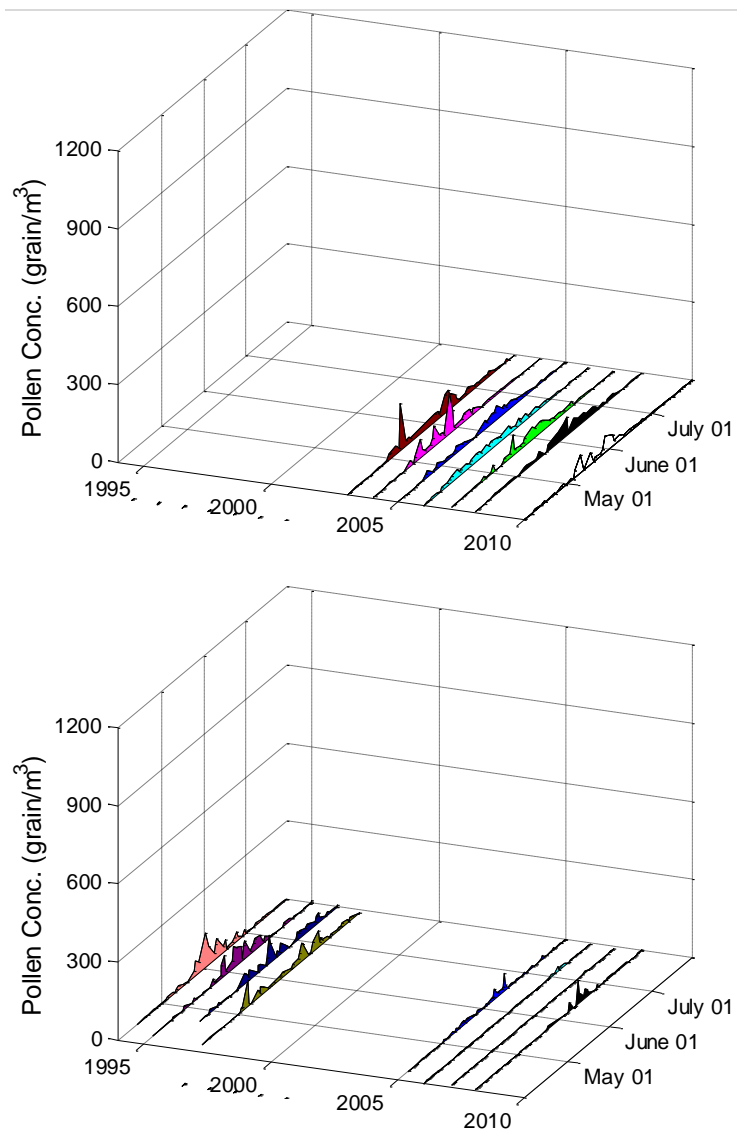


Figure 13. Time series of observed daily pollen concentration of Gramineae in Cherry Hill, NJ (top) and Newark, NJ (bottom) monitor stations which are located in the Northeast. The pollen data are from Dr. Leonard, Bielory.

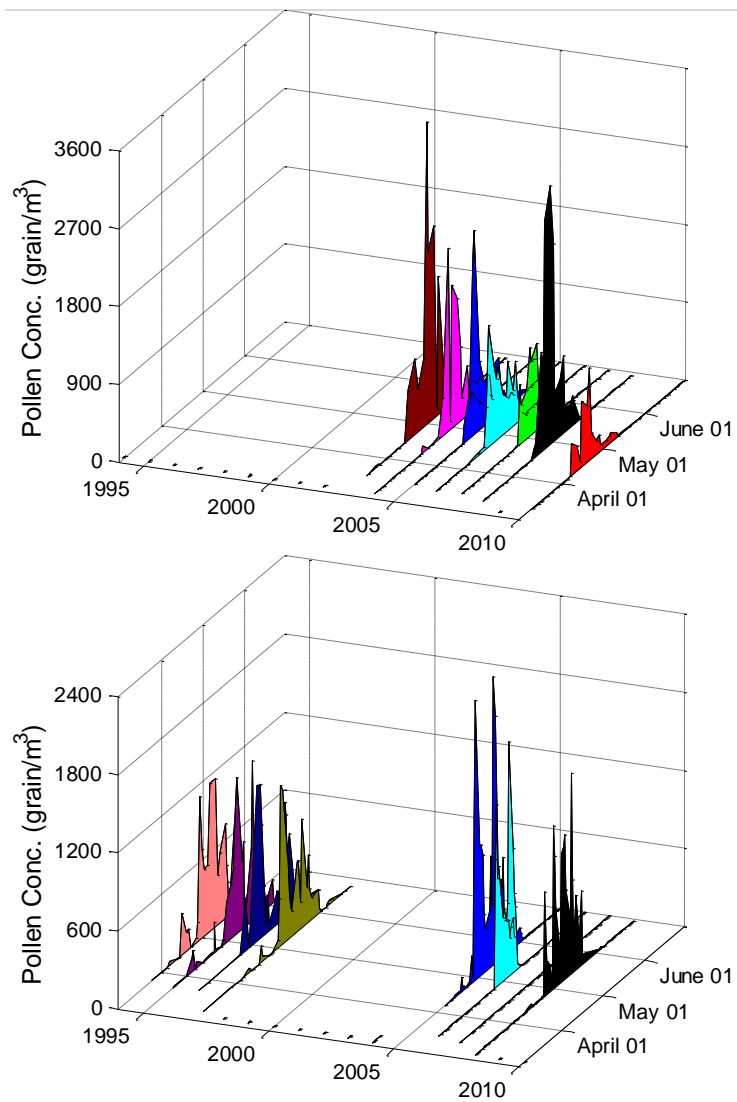


Figure 14. Time series of observed daily pollen concentration of *Quercus* in Cherry Hill, NJ (top) and Newark, NJ (bottom) monitor stations which are located in the Northeast. The pollen data are from Dr. Leonard, Bielory.

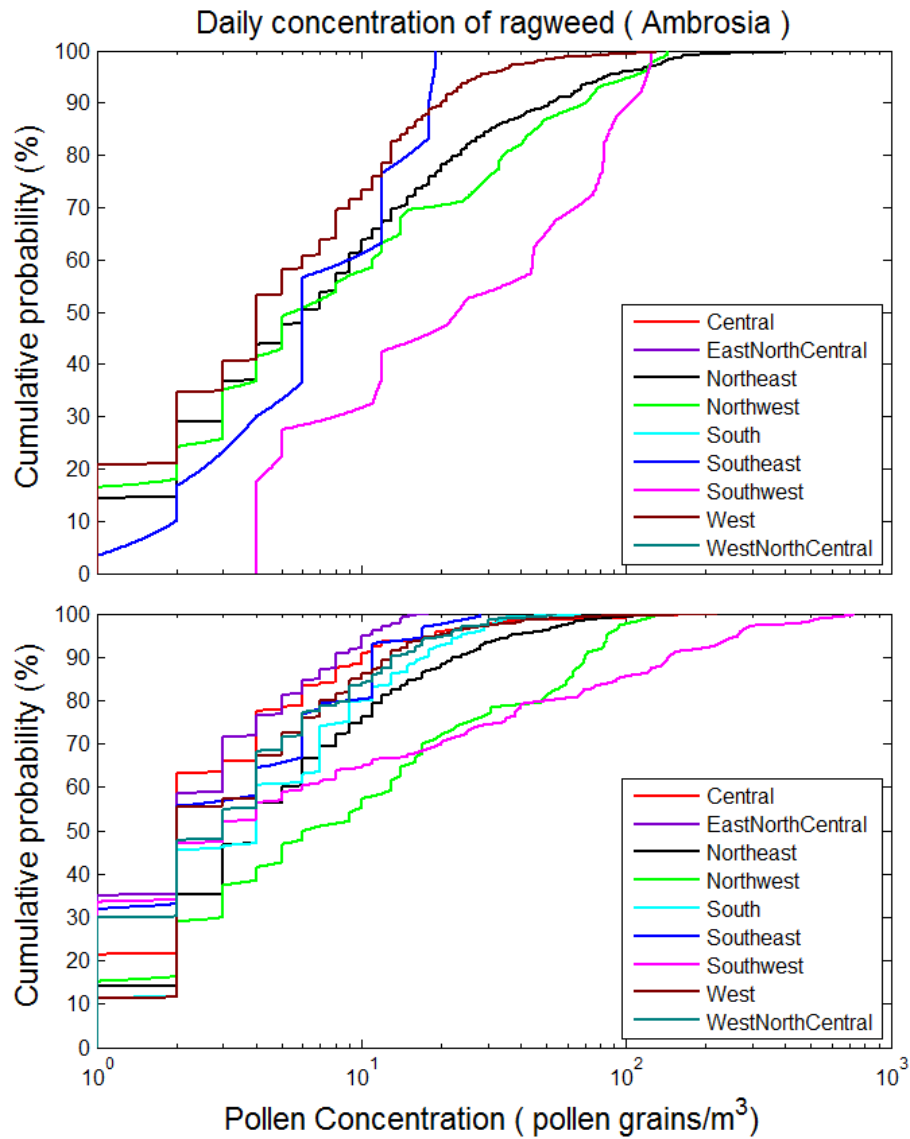


Figure 15. Cumulative probability distributions of observed airborne daily pollen concentration for Ambrosia in the nine climate regions of contiguous US in 1994-2000 (top) and 2003-2010 (bottom).

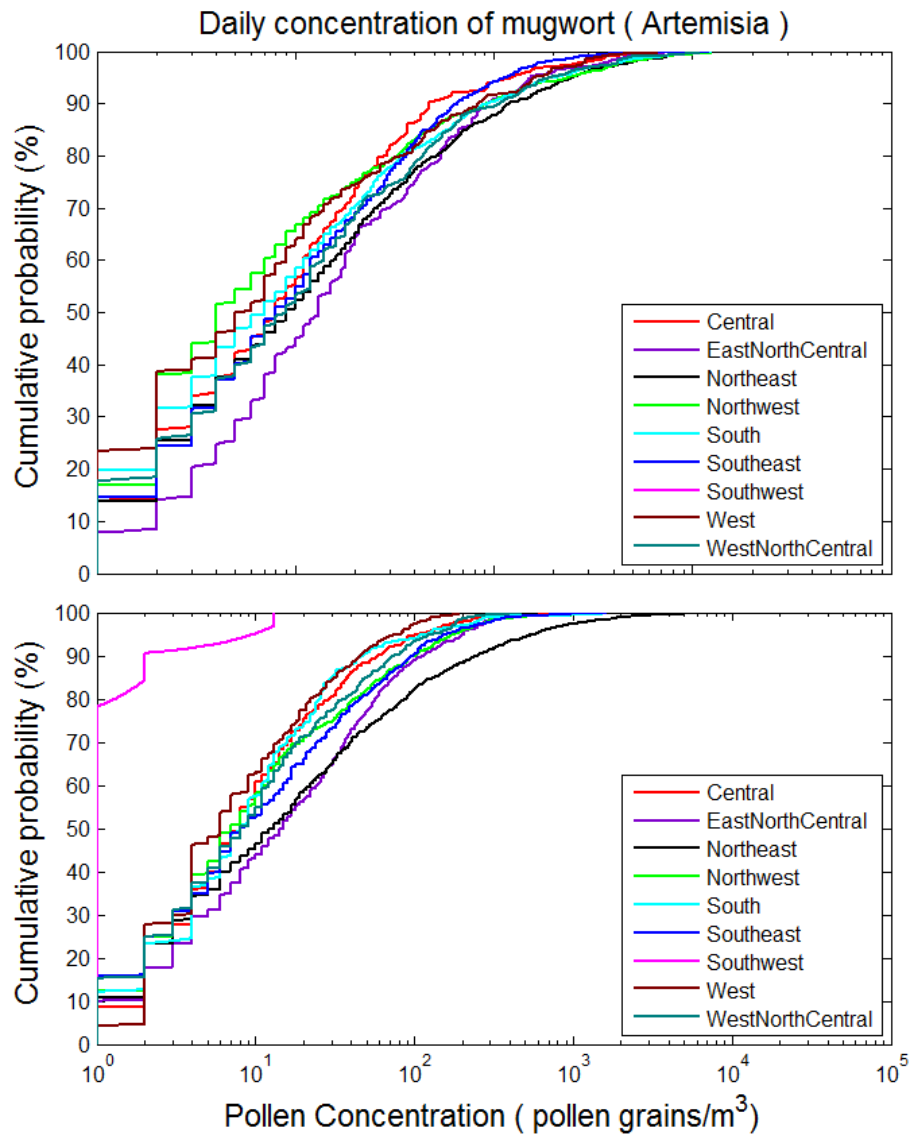


Figure 16. Cumulative probability distributions of observed airborne daily pollen concentration for *Artemisia* in the nine climate regions of contiguous US in 1994-2000 (top) and 2003-2010 (bottom).

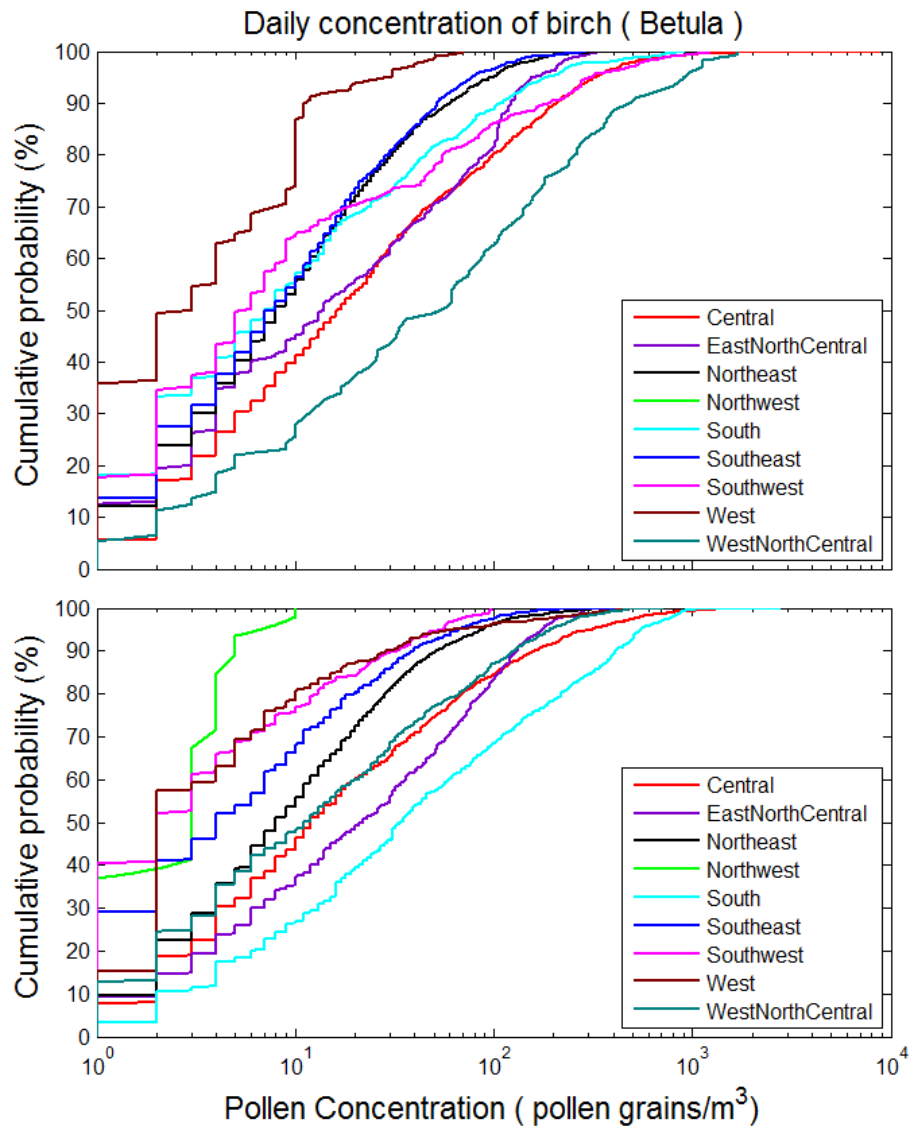


Figure 17. Cumulative probability distributions of observed airborne daily pollen concentration for Betula in the nine climate regions of contiguous US in 1994-2000 (top) and 2003-2010 (bottom)

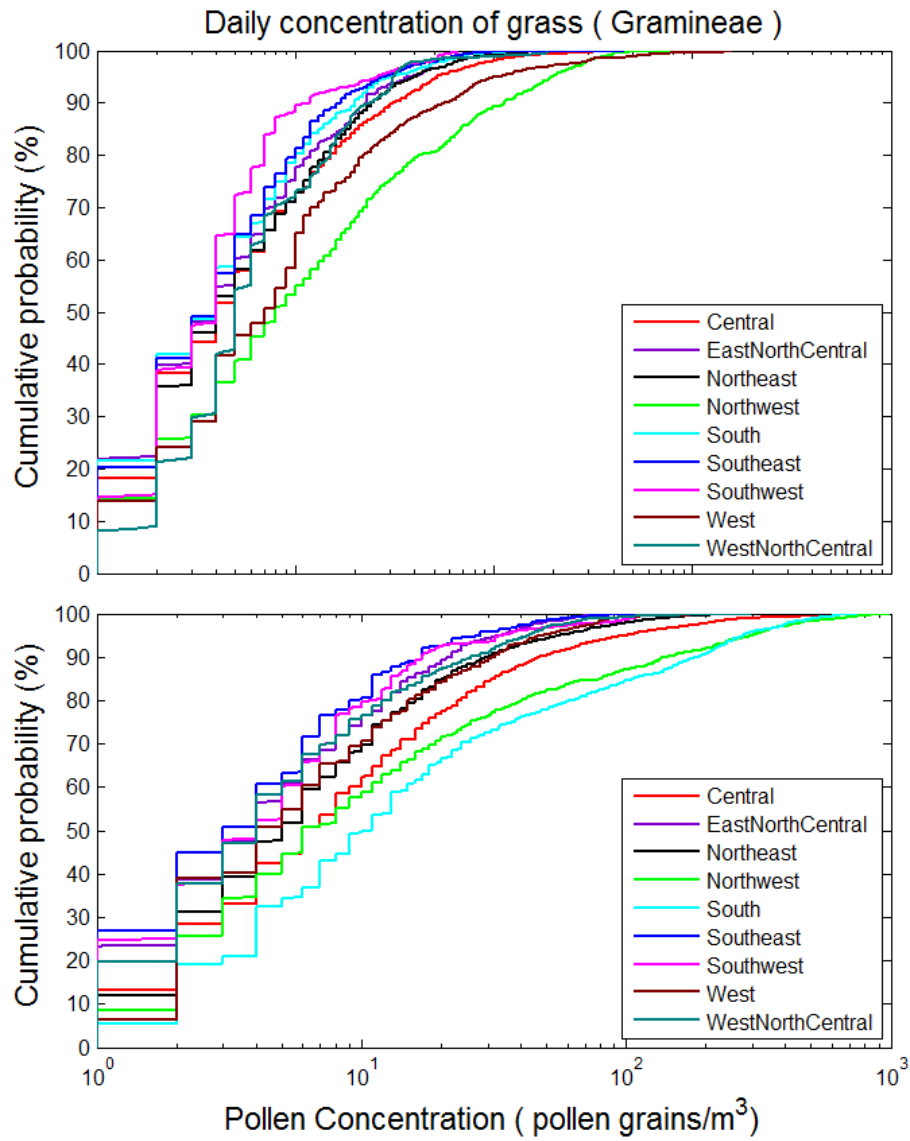


Figure 18. Cumulative probability distributions of observed airborne daily pollen concentration for Gramineae in the nine climate regions of contiguous US in 1994-2000 (top) and 2003-2010 (bottom)

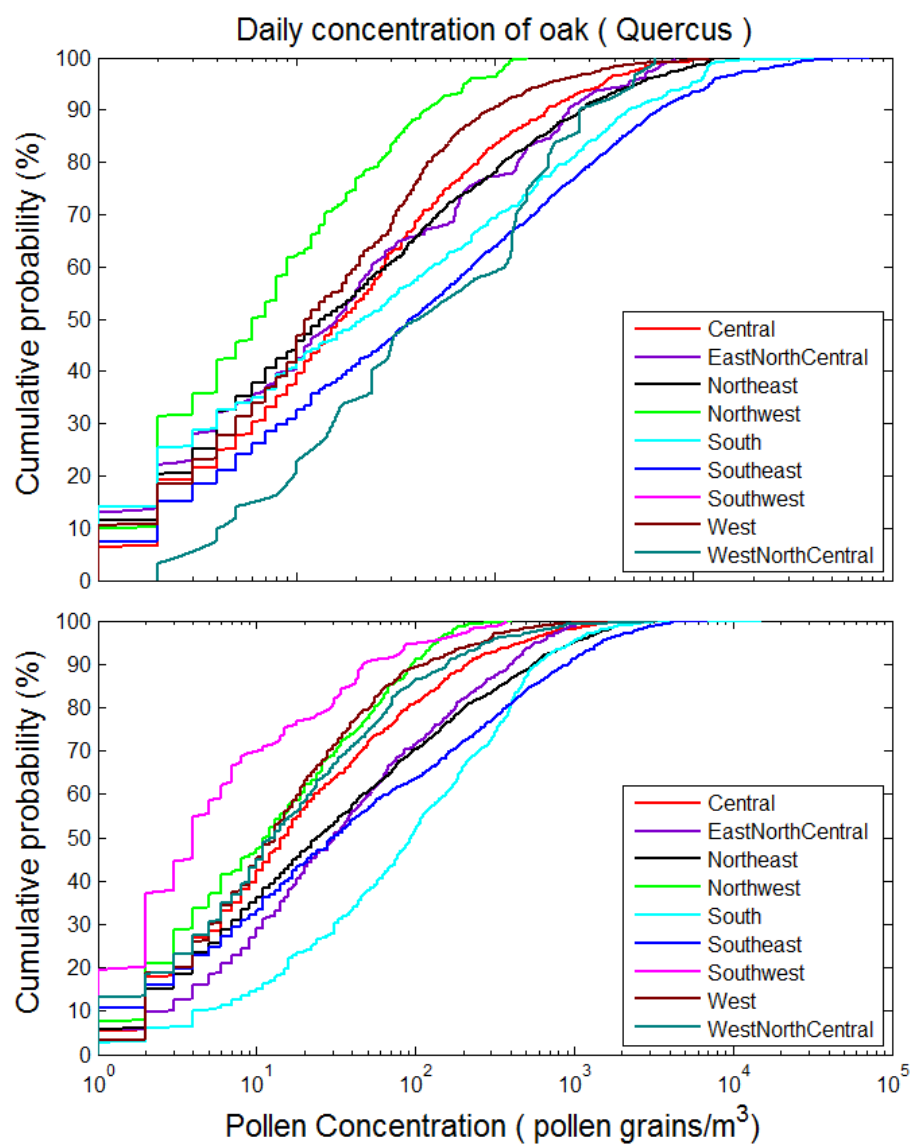


Figure 19. Cumulative probability distributions of observed airborne daily pollen concentration for *Quercus* in the nine climate regions of contiguous US in 1994-2000 (top) and 2003-2010 (bottom)

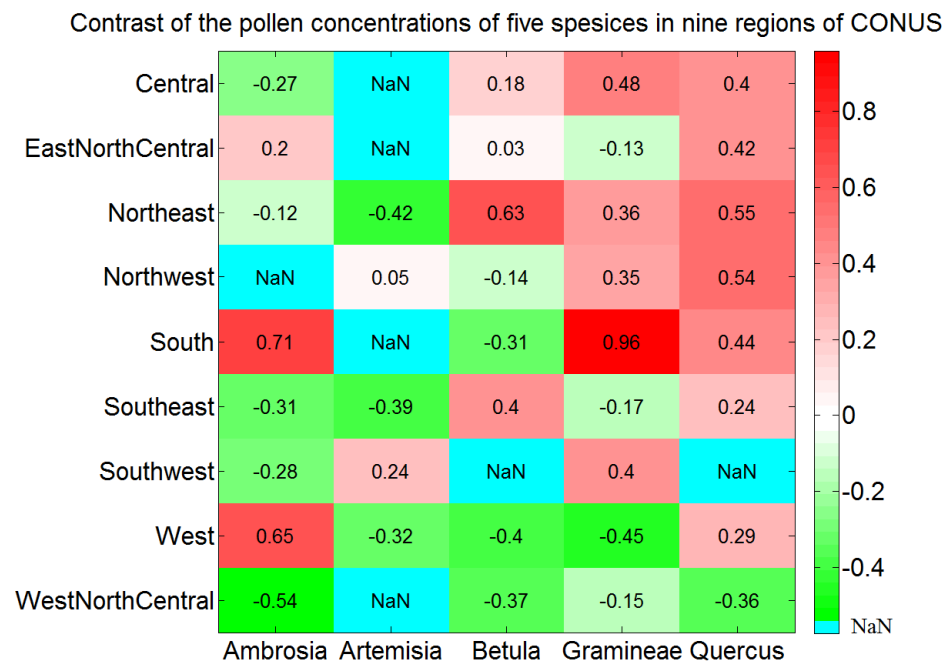


Figure 20 The heat map shows the trend of the mean daily concentrations of pollen of five species in nine climate regions of CONUS. The values shown in heat map are the standardized logarithmic values. Larger values are redder, indicating great increasing of daily concentrations in the second year period (2003-2010). Smaller values are greener, indicating great decreasing of daily concentrations in the second year period (2003-2010). Blue box shows that there is no data in that region for that species in period 1994-2000

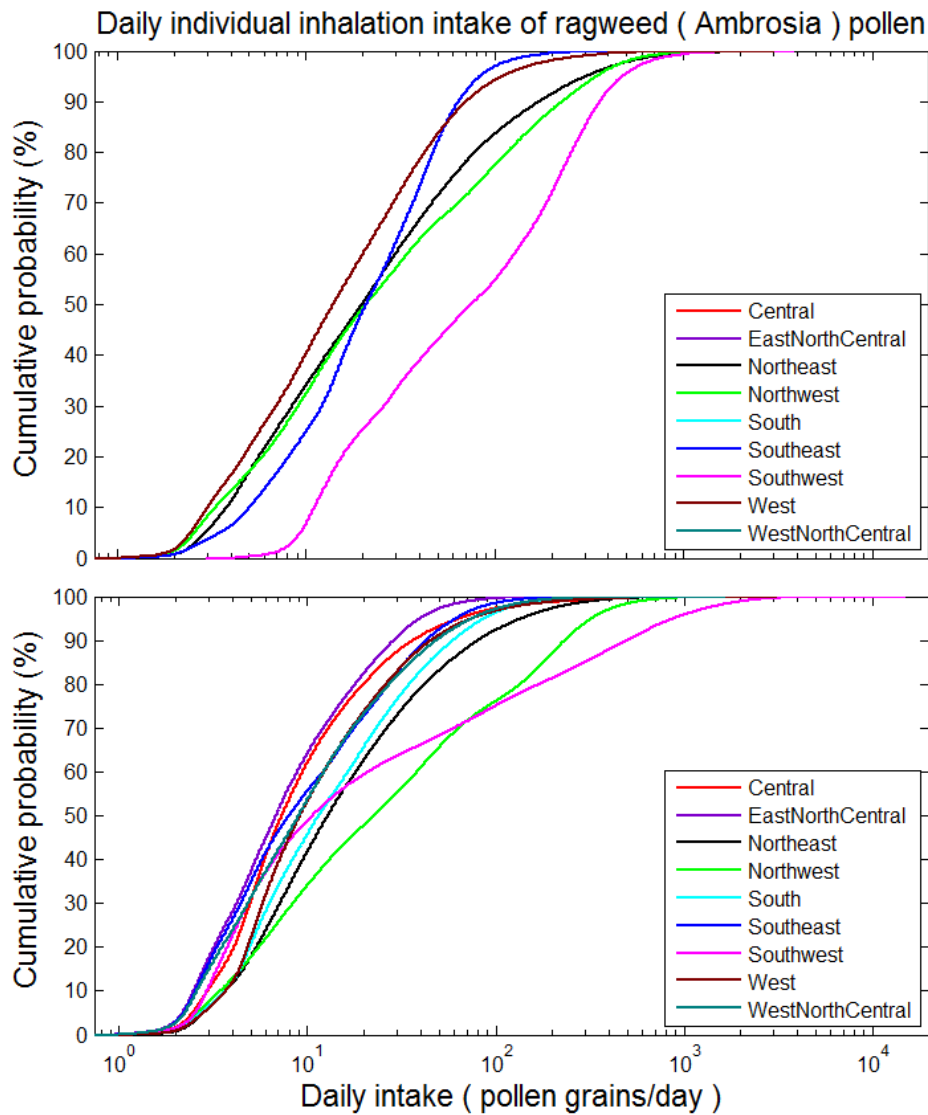


Figure 21. Simulated cumulative probability distribution of daily intake via inhalation of Ambrosia pollen in the different climate regions in 1994-2000 (top) and 2003-2010 (bottom). Estimates were from simulation results of 100,000 virtual individuals in each climate region, considering the inhalation exposure route.

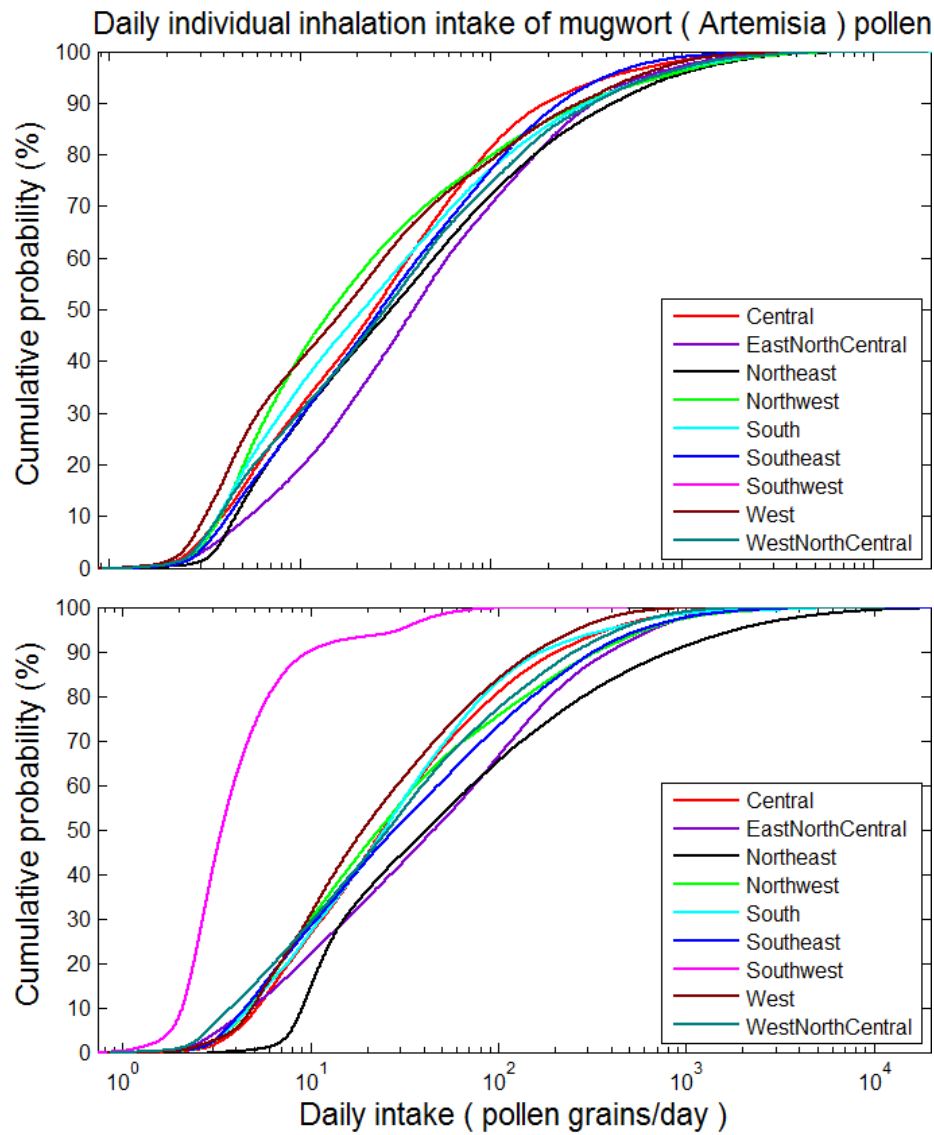


Figure 22. Simulated cumulative probability distribution of daily intake via inhalation of *Artemisia* pollen in the different climate regions in 1994-2000 (top) and 2003-2010 (bottom). Estimates were from simulation results of 100,000 virtual individuals in each climate region, considering the inhalation exposure route.

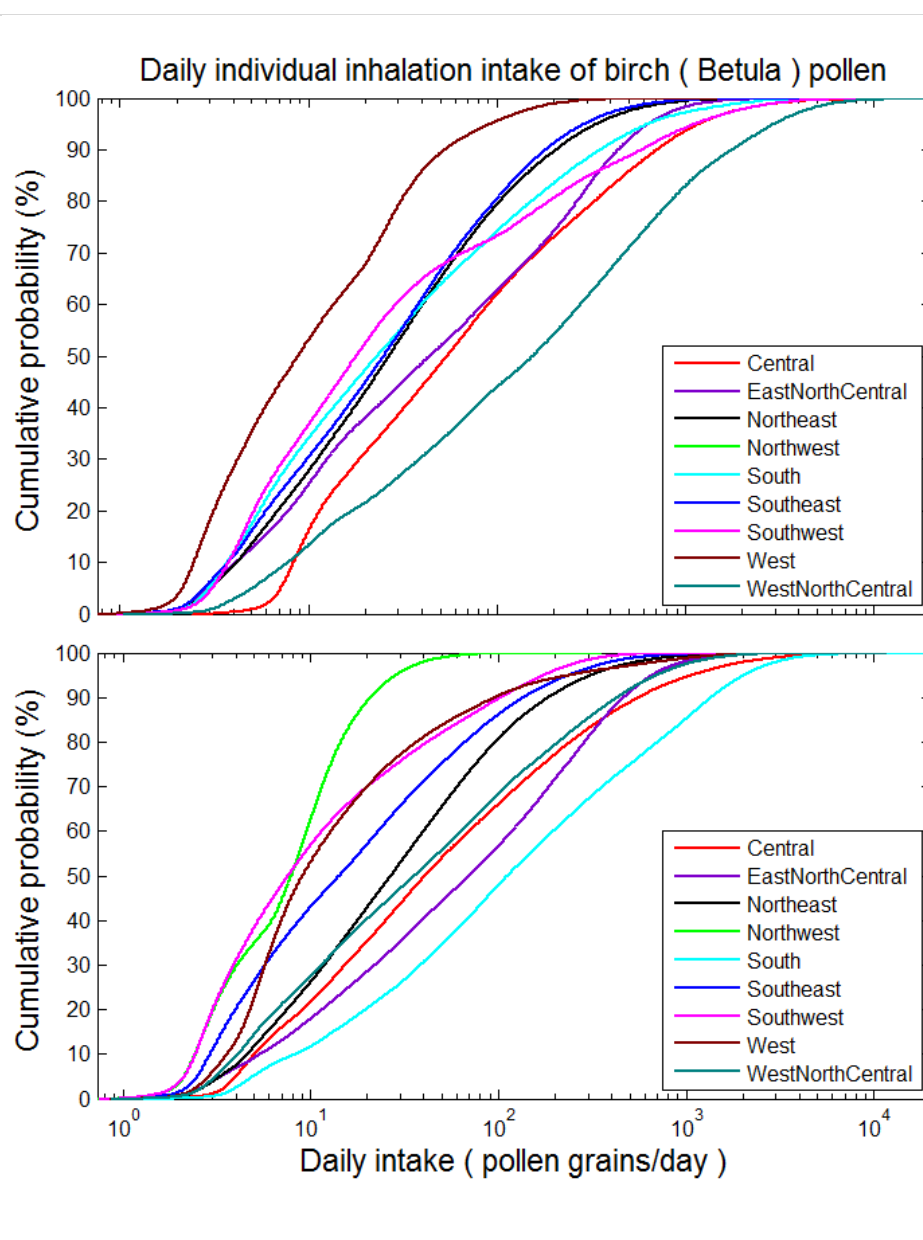


Figure 23. Simulated cumulative probability distribution of daily intake via inhalation of Betula pollen in the different climate regions in 1994-2000 (top) and 2003-2010 (bottom). Estimates were from simulation results of 100,000 virtual individuals in each climate region, considering the inhalation exposure route.

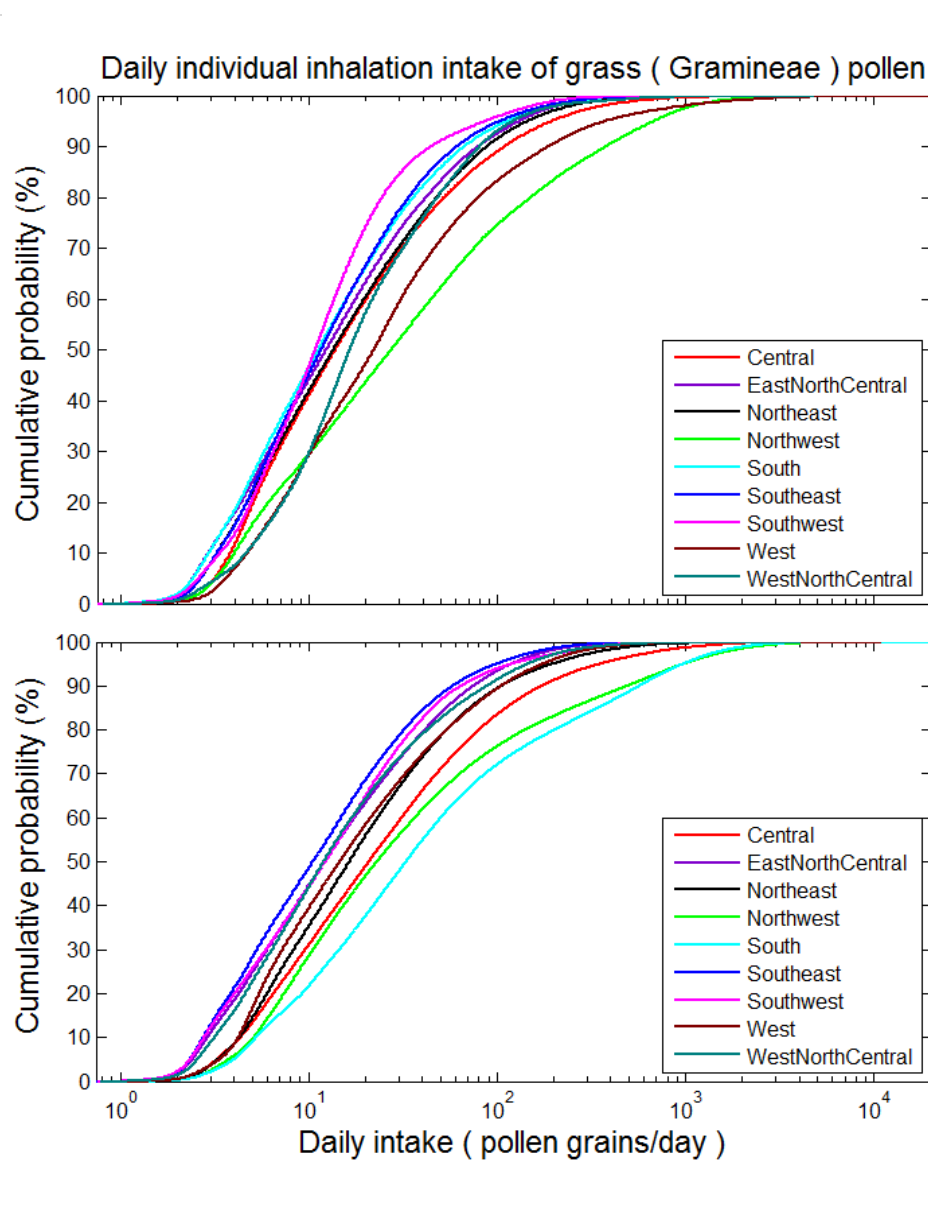


Figure 24. Simulated cumulative probability distribution of daily intake via inhalation of Gramineae pollen in the different climate regions in 1994-2000 (top) and 2003-2010 (bottom). Estimates were from simulation results of 100,000 virtual individuals in each climate region, considering the inhalation exposure route.

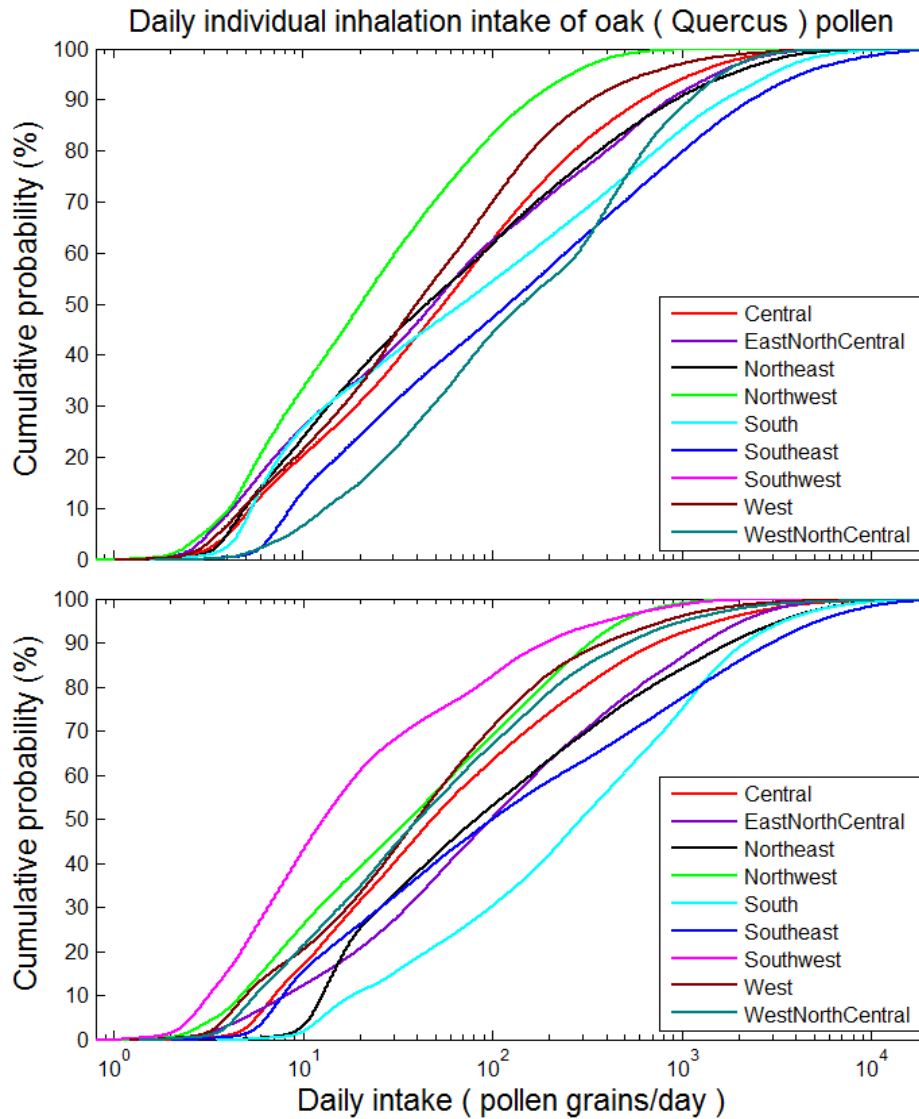


Figure 25. Simulated cumulative probability distribution of daily intake via inhalation of *Quercus* pollen in the different climate regions in 1994-2000 (top) and 2003-2010 (bottom). Estimates were from simulation results of 100,000 virtual individuals in each climate region, considering the inhalation exposure route.

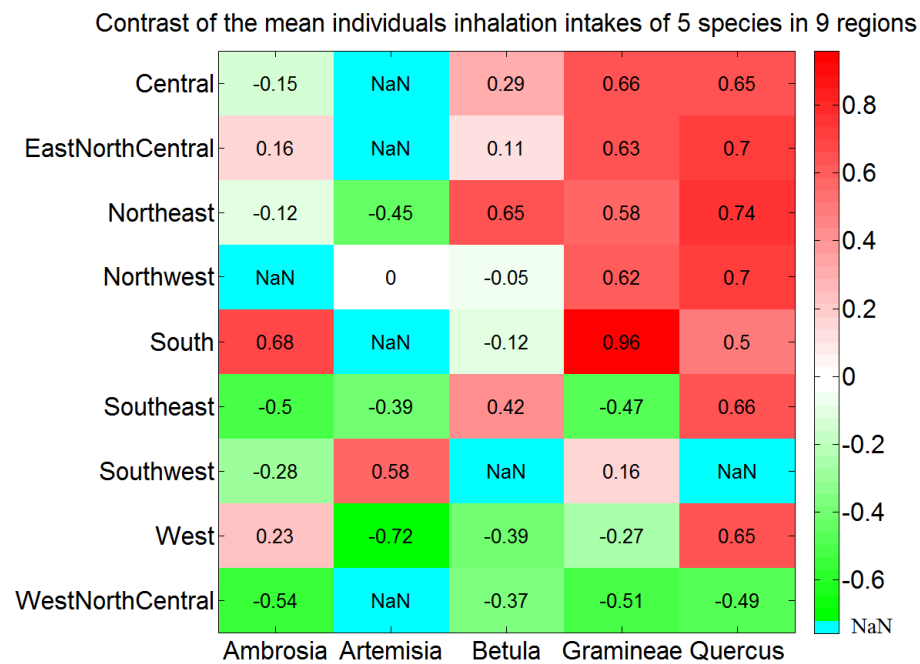


Figure 26 The heat map shows the trend of the mean daily inhalation intakes of “virtual individuals” of the population of pollen of five species in nine climate regions of CONUS. The values shown in heat map are the standardized logarithmic values. Larger values are redder, indicating great increasing of daily concentrations in the second year period (2003-2010). Smaller values are greener, indicating great decreasing of daily concentrations in the second year period (2003-2010). Blue box shows that there is no data in that region for that species in period 1994-2000

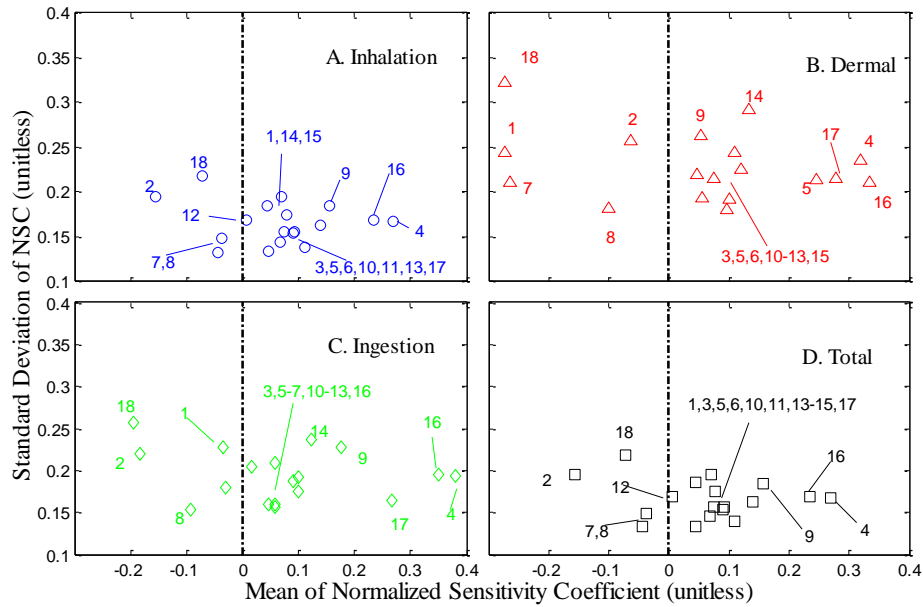


Figure 27. Mean and Standard Deviation of Normalized Sensitivity Coefficient (NSC) for population exposure in Central Climate Region: (A) Inhalation, (B) Dermal, (C) Ingestion, (D) Total Exposures. The vertical dashed lines represent the NSC values of 0. Numbers in the figure are parameter IDs: 1 u^* friction velocity (m/s), 2 k von karman constant (dimensionless), 3 D_p diameter of pollen (m), 4 P_p density of pollen (kg/m³), 5 μ viscosity of air (m/s), 6 T temperature (k), 7 P_a density of air (kg/m³), 8 T_{ind} indoor time (day), 9 T_{out} outdoor time (day), 10 F_r hand to mouth contact frequency (time/hour), 11 Sa_f female surface area (m²), 12 Sa_m human surface area (m²), 13 R_h hand surface ratio (%), 14 In_f female inhalation rate (m³/day), 15 In_m male inhalation rate (m³/day), 16 λ_v indoor ventilation rate (s⁻¹), 17 L_r derm loading rate (dimensionless), 18 R_m removal coefficient on the skin (dimensionless). (see

[Table 2](#) for details)

带格式的: 检查拼写和语法

7 Tables

Table 1. Coordinates, elevation, main climate characteristics of the studied AAAAI pollen monitoring stations.

Station Name	Lat (N)	Lon (W)	Elevation	Climate Region	Mean Temp
Corpus Christi, TX	27.8	97.4	2	South	22.21
Tampa, FL	28.06	82.43	12	Southeast	22.73
Tallahassee, FL	30.44	84.28	62	Southeast	19.67
Georgetown, TX	30.64	96.31	91	South	19.48
College Station, TX	30.64	97.76	269	South	20.31
Waco, TX	31.51	97.2	185	South	19.44
Dallas, TX	33.04	96.83	207	South	19.29
Scottsdale, AZ	33.49	111.92	377	Southwest	23.98
Orange, CA	33.78	117.86	53	West	17.93
Atlanta, GA	33.97	84.55	366	Southeast	16.83
Santa Barbara, CA	34.44	119.76	57	West	14.86
Huntsville, AL	34.73	86.59	191	Southeast	16.26
Little Rock, AR	34.75	92.39	115	South	17.28
Charlotte, NC	35.3	80.75	229	Southeast	16.02
Fort Smith, AR	35.35	94.39	186	South	16.49
Oklahoma City, OK	35.61	97.6	340	South	15.90
Los Alamos, NM	35.88	106.32	2227	Southwest	11.80
Knoxville, TN	35.95	84.01	305	Central	15.01
Tulsa 1, OK	36.03	95.87	207	South	16.17

Station Name	Lat (N)	Lon (W)	Elevation	Climate Region	Mean Temp
Durham, NC	36.05	78.9	110	Southeast	15.71
Las Vegas, NV	36.17	115.15	620	West	20.93
San Jose 2, CA	37.31	121.97	47	West	15.69
San Jose 2, CA	37.33	121.94	35	West	15.69
Pleasanton, CA	37.69	121.91	100	West	14.18
Lexington, KY	38.04	84.5	299	Central	13.11
Roseville, CA	38.76	121.27	57	West	16.96
Colorado Springs 2, CO	38.87	104.82	1867	Southwest	9.75
Colorado Springs 1, CO	38.87	104.83	1868	Southwest	9.64
Kansas City, MO	39.08	94.58	288	Central	13.91
Baltimore, MD	39.37	76.47	36	Northeast	13.33
Reno, NV	39.56	119.77	1382	West	12.08
New Castle, DE	39.66	75.57	3	Northeast	13.46
Indianapolis, IN	39.91	86.2	254	Central	11.98
York, PA	39.94	74.91	13	Northeast	12.72
Cherry Hill, NJ	39.94	76.71	195	Northeast	13.04
Philadelphia, PA	39.96	75.16	12	Northeast	13.46
Pittsburgh, PA	40.47	79.95	287	Northeast	11.20
Newark, NJ	40.74	74.19	43	Northeast	13.02
Lincoln, NE	40.82	96.64	371	West North Central	11.03
Armonk, NY	41.13	73.73	187	Northeast	11.09
Omaha, NE	41.14	95.97	305	West North Central	10.95
Waterbury, CT	41.55	73.07	140	Northeast	11.83
Chicago, IL	41.91	87.77	189	Central	11.03
Olean, NY	42.09	78.43	433	Northeast	7.30

Station Name	Lat (N)	Lon (W)	Elevation	Climate Region	Mean Temp
Erie, PA	42.1	80.13	215	Northeast	10.12
Salem, MA	42.5	70.92	42	Northeast	10.90
St. Clair Shores, MI	42.51	82.9	180	East North Central	9.82
Twin Falls, ID	42.58	114.46	1124	Northwest	10.23
Chelmsford, MA	42.6	71.35	37	Northeast	10.01
Albany, NY	42.68	73.77	72	Northeast	9.41
London, ON, Canada	42.99	81.25	250	Central	8.34
Waukesha, WI	43.02	88.24	270	East North Central	9.60
Madison, WI	43.08	89.43	263	East North Central	8.66
Niagara Falls, ON ,	43.09				
Canada		79.09	188	Northeast	9.27
Rochester, NY	43.1	77.58	148	Northeast	9.33
LaCrosse, WI	43.88	91.19	216	East North Central	8.96
Eugene, OR	44.04	123.09	129	Northwest	11.35
Vancouver, WA	45.62	122.5	89	Northwest	12.25
Fargo, ND	46.84	96.87	277	West North Central	5.89
Seattle, WA	47.66	122.29	20	Northwest	11.94

Table 2. Parameters for calculating population exposure to pollen in nine different climate regions in CONUS. These parameters were listed either as fixed values, known distributions, or unknown empirical distributions derived from the literature (Sofiev et al., 2013).

Parameter	ID	Distribution	Range	Reference
u^* friction velocity (m/s)	1	fixed	-	(Helbig et al., 2004)
K_{von} karman constant (dimensionless)	2	fixed	-	(Sofiev et al., 2013)
D_p diameter of pollen (m)	3	fixed	-	(Cohen et al., 1979)
P_p density of pollen (kg/m ³)	4	fixed	-	(Sofiev et al., 2013)
μ viscosity of air (m/s)	5	fixed	-	(Helbig et al., 2004)
T_a temperature (K)	6	range	283-310	(Seinfeld & Pandis, 2012)
P_a density of air (kg/m ³)	7	fixed	-	(Seinfeld & Pandis, 2012)

带格式表格

Parameter	ID	Distribution	Range	Reference
<u>T_{ind} indoor</u>				(USEPA, 2010)
<u>time (day)</u>	8	norm	-	
<u>T_{out} outdoor</u>				(USEPA, 2010)
<u>time (day)</u>	9	norm	-	
<u>F_r hand to</u>				(USEPA, 2010)
<u>mouth</u>				
<u>contact</u>				
<u>frequency</u>				
<u>(time/hour)</u>	10	empirical	23.0-58.0	
<u>S_{af} female</u>				(USEPA, 2010)
<u>surface area</u>				
<u>(m²)</u>	11	lognorm	0.41-2.51	
<u>S_{am} male</u>				(USEPA, 2010)
<u>surface area</u>				
<u>(m²)</u>	12	lognorm	0.41-2.51	
<u>R_h hand</u>				(USEPA, 2010)
<u>surface ratio</u>				
<u>(%)</u>	13	lognorm	4.8-5.6	
<u>lh_f female</u>				(USEPA, 2010)
<u>inhalation</u>				
<u>rate (m³/day)</u>	14	uniform	0.19-1.91	
<u>lh_m male</u>				(USEPA, 2010)
<u>inhalation</u>				
<u>rate (m³/day)</u>	15	uniform	0.20-1.50	

带格式表格

Parameter	ID	Distribution	Range	Reference
$\Delta v_{\text{indoor ventilation rate (hour}^{-1}\text{)}}$	16	empirical	0.2-2	(Helbig et al., 2004)
$Lr_{\text{efficiency of adherence (dimensionless)}}$	17	empirical		(Fogh & Andersson, 2000)
$R_{m\text{removal coefficient on the skin (dimensionless)}}$	18	empirical	10.0-25.0	(Cohen et al., 1930)

带格式表格

Table 3. Median and mean (\pm standard deviation) of the exposure in Northeast climate region through different exposure routes (pollen grains/day) in 1994-2000

Species	Median or Mean	Inhalation	Dermal Contact	Ingestion	Total
birch (Betula)	Median	30	0	0	30
	Mean	206(821)	2(8)	2(7)	208
ragweed (Ambrosia)	Median	28	0	0	28
	Mean	86(206)	1(1)	0(1)	87
mugwort (Artemisia)	Median	20	0	0	20
	Mean	85(489)	0(2)	0(1)	85
grass (Gramineae)	Median	13	0	0	13
	Mean	38(86)	0(1)	0(1)	0
oak (Quercus)	Median	45	1	0	45
	Mean	386(1112)	3(7)	2(5)	390

Table 4. Comparisons of mean peak values between periods 1994-2000 and 2003-2010. Red values indicate that those species in those regions vary significantly over time.

Species	ragweed (<i>Ambrosia</i>)			mugwort (<i>Artemisia</i>)			birch (<i>Betula</i>)			grass (<i>Gramineae</i>)			oak (<i>Quercus</i>)		
	1994-2000	2003-2010	Diff.	1994-2000	2003-2010	Diff.	1994-2000	2003-2010	Diff.	1994-2000	2003-2010	Diff.	1994-2000	2003-2010	Diff.
Central	705	397	308		34	-34	196	215	-18	109	198	-89	349	662	-313
EastNorthCentral	185	215	-29		10	-10	250	232	18	51	50	1	461	741	-281
Northeast	123	103	19	136	56	79	438	1052	-613	84	144	-60	730	1576	-847
Northwest		4	-4	143	30	114	443	399	44	269	392	-123	74	127	-53
South	271	556	-286		21	-21	378	183	196	47	203	-156	1220	1654	-434
Southeast	118	105	13	8	7	1	191	265	-73	71	53	18	1799	2326	-527
Southwest	441	38	403	124	159	-35		3	-3	40	43	-3	82	192	-192
West	32	34	-2	53	21	32	190	47	143	738	63	675	348	309	39
WestNorthCentral	1053	319	734		22	-22	349	185	164	110	83	27	456	693	-237

Table 5. Comparisons of mean of pollen concentrations between periods 1994-2000 and 2003-2010.. Red values indicate that those species in those regions vary significantly over time.

	ragweed (<i>Ambrosia</i>)			mugwort (<i>Artemisia</i>)			birch (<i>Betula</i>)			grass (<i>Gramineae</i>)			oak (<i>Quercus</i>)		
	1994-2000	2003-2010	Diff.	1994-2000	2003-2010	Diff.	1994-2000	2003-2010	Diff.	1994-2000	2003-2010	Diff.	1994-2000	2001-2010	Diff.
Central	79	65	14		6	-6	27	30	-2	14	23	-10	69	99	-30
EastNorthCentral	43	48	-4		3	-3	41	41	0	9	8	0	82	123	-41
Northeast	22	21	1	19	10	10	52	129	-77	10	14	-4	97	193	-96
Northwest		3	-3	21	22	0	43	41	2	37	50	-12	17	33	-16
South	41	129	-88		7	-7	41	31	10	8	53	-45	165	257	-91
Southeast	20	15	5	8	5	4	27	39	-12	8	7	1	256	293	-37
Southwest	60	10	50	41	47	-6		2	-2	6	9	-3	12	23	-23
West	7	17	-11	9	6	2	31	17	14	965	12	953	46	55	-10
WestNorthCentral	173	43	131		6	-6	43	27	16	10	10	1	113	74	39

Table 6. Median and range of the inhalation intakes in nine climate regions of contiguous US 1994-2000(pollen grains/day)

Species	Percentile	East North		North		
		Central	Central	East	North West	South
birch (Betula)	25%	15	10	9	NaN	7
	50%					
	(Median)	53	42	28	NaN	23
	75%	231	203	82	NaN	104
	95%	1173	654	347	NaN	663
ragweed						
(Ambrosia)	25%	NaN	NaN	7	7	NaN
	50%					
	(Median)	NaN	NaN	20	21	NaN
	75%	NaN	NaN	61	86	NaN
	95%	NaN	NaN	313	338	NaN
mugwort						
(Artemisia)	25%	7	14	8	6	7
	50%					
	(Median)	24	40	30	15	21
	75%	69	126	119	64	82
	95%	416	565	857	712	622
grass						
(Gramineae)	25%	6	5	6	8	5
	50%					
	(Median)	13	12	13	25	11

Species	Percentile	East North		North		South
		Central	Central	East	North West	
	75%	38	31	37	97	28
	95%	194	122	149	653	121
oak (Quercus)	25%	14	9	11	7	10
	50%					
	(Median)	56	47	45	21	68
	75%	198	262	249	64	506
	95%	1141	1451	1803	256	3057
Species	Percentile	South		West North		US
		East	South West	West	Central	
birch (Betula)	25%	8	6	4	26	10
	50%					
	(Median)	25	17	9	149	43
	75%	73	123	25	607	181
	95%	286	1101	89	2970	910
ragweed						
(Ambrosia)	25%	10	18	6	NaN	10
	50%					
	(Median)	21	68	14	NaN	29
	75%	41	214	33	NaN	87
	95%	82	456	109	NaN	259
mugwort						
(Artemisia)	25%	8	NaN	5	8	8
	50%					
	(Median)	26	NaN	17	28	25

Species	Percentile	East North		North		
		Central	Central	East	North West	South
	75%	90	NaN	70	102	90
	95%	402	NaN	526	642	593
grass						
(Gramineae)	25%	5	5	8	9	6
	50%					
	(Median)	11	11	22	16	15
	75%	27	20	60	37	42
	95%	100	82	383	114	213
oak (Quercus)	25%	21	NaN	13	12	15
	50%					
	(Median)	129	NaN	40	39	68
	75%	753	NaN	122	159	333
	95%	4291	NaN	796	1087	1781

Table 7. Median and range of the inhalation intakes in nine climate regions of contiguous US in 2003-2010 (pollen grains/day)

Species	Percentile	East North		North		
		Central	Central	East	North West	South
birch (Betula)	25%	5	4	6	7	6
	50%					
	(Median)	7	7	13	23	11
	75%	15	14	33	85	27
	95%	59	40	135	320	87
ragweed (Ambrosia)	25%	12	15	9	3	28
	50%					
	(Median)	39	68	26	8	109
	75%	173	222	77	13	472
	95%	1035	654	306	29	1951
mugwort (Artemisia)	25%	9	12	13	8	9
	50%					
	(Median)	24	44	42	23	25
	75%	70	150	188	92	66
	95%	385	673	1903	615	421
grass (Gramineae)	25%	8	5	7	9	11
	50%					
	(Median)	21	12	16	24	33
	75%	58	33	42	91	130

Species	Percentile	East North		North		South
		Central	Central	East	North West	
	95%	312	119	198	956	940
oak (Quercus)	25%	15	26	20	9	68
	50%					
	(Median)	47	100	82	36	292
	75%	210	444	470	134	968
	95%	1467	2053	3476	479	3534
Species	Percentile	South		West North		US
		East	South West	West	Central	
birch (Betula)	25%	5	3	5	9	10
	50%					
	(Median)	14	7	9	35	35
	75%	50	28	26	145	134
	95%	232	172	215	670	585
ragweed (Ambrosia)	25%	4	4	5	4	5
	50%					
	(Median)	8	11	9	9	11
	75%	21	98	21	22	37
	95%	59	867	74	70	190
mugwort (Artemisia)	25%	9	2	8	8	9
	50%					
	(Median)	29	3	18	26	26
	75%	106	5	58	84	91
	95%	582	29	272	438	591

Species	Percentile	East North		North		
		Central	Central	East	North West	South
grass						
(Gramineae)	25%	4	5	6	5	7
	50%					
	(Median)	10	12	14	12	17
	75%	26	30	40	33	54
	95%	98	124	169	148	340
oak (Quercus)	25%	18	5	13	37	21
	50%					
	(Median)	101	13	41	137	83
	75%	892	53	127	503	384
	95%	5413	387	651	1601	2077

Table 8. Mean and standard deviation of the individual inhalation intake values in 9 climate regions in 1994-2000 (pollen grains/day)

	East North		North		
Species	Central	Central	East	North West	South
birch (Betula)	100 (294)	151 (420)	206 (821)	167 (976)	151 (625)
ragweed					
(Ambrosia)	320 (1554)	163 (331)	86 (206)		161 (677)
mugwort					
(Artemisia)			85 (489)	79 (151)	
grass (Gramineae)	54 (246)	31 (64)	38 (86)	137 (404)	30 (64)
					641
oak (Quercus)	274 (1202)	302 (798)	366 (1112)	61 (128)	(2083)
	South	South West	West North		
Species	East		West	Central	US
birch (Betula)	103 (367)		111 (322)	176 (1109)	146 (616)
ragweed					
(Ambrosia)	73 (159)	219 (743)	24 (68)	664 (1764)	213 (687)
mugwort					
(Artemisia)	30 (33)	146 (206)	32 (87)		74 (193)
grass (Gramineae)	83 (290)	31 (67)	54 (194)	196 (719)	72 (237)
			801		401
oak (Quercus)	401 (2173)	464 (1073)	(3990)	120 (241)	(1312)

Table 9. Mean and standard deviation of the individual inhalation intakes in 9 climate regions in 2003-2010 (pollen grains/day)

Species	East North		North		South
	Central	Central	East	North West	
birch (Betula)	121 (731)	155 (345)	541 (3182)	166 (715)	146 (1063)
ragweed (Ambrosia)	302 (2534)	173 (287)	83 (242)	10 (12)	461 (1074)
mugwort (Artemisia)	20 (69)	12 (18)	34 (76)	79 (144)	25 (57)
grass (Gramineae)	83 (290)	31 (67)	54 (194)	196 (719)	72 (237)
oak (Quercus)	401 (2173)	464 (1073)	214 (972)	316 (1920)	401 (1312)
Species	South		South West		West North
	East	West	Central	US	
birch (Betula)	156 (635)	7 (15)	65 (158)	112 (511)	163 (780)
ragweed (Ambrosia)	17 (26)	175 (562)	24 (87)	20 (39)	162 (540)
mugwort (Artemisia)	124 (263)	321 (452)	105 (497)	369 (984)	121 (284)
grass (Gramineae)	27 (64)	33 (95)	44 (111)	38 (128)	114 (368)
oak (Quercus)	1109 (2856)	84 (291)	801 (3990)	120 (241)	667 (1974)

8 Appendix



- (a) ragweed (*Ambrosia*)
- (b) mugwort (*Artemisia*)
- (c) birch (*Betula*)
- (d) grasses (*Gramineae*)
- (e) oak (*Quercus*)

9 References

- Behrendt, H., and Becker, W.-M. 2001. Localization, release and bioavailability of pollen allergens: the influence of environmental factors. *Current Opinion in Immunology* 13 (6):709-715.
- Bielory, L., Lyons, K., and Goldberg, R. 2012. Climate change and allergic disease. *Current allergy and asthma reports* 12 (6):485-494.
- Björkstén, F., Suoniemi, I., and Koski, V. 1980. Neonatal birch - pollen contact and subsequent allergy to birch pollen. *Clinical & Experimental Allergy* 10 (5):585-591.
- Brożek, J.L., Bousquet, J., Baena-Cagnani, C.E., Bonini, S., Canonica, G.W., Casale, T.B., van Wijk, R.G., Ohta, K., Zuberbier, T., and Schünemann, H.J. 2010. Allergic Rhinitis and its Impact on Asthma (ARIA) guidelines: 2010 revision. *Journal of Allergy and Clinical Immunology* 126 (3):466-476.
- Chivato, T., Juan, F., Montoro, A., and Laguna, R. 1996. Anaphylaxis induced by ingestion of a pollen compound. *Journal of investigational allergology & clinical immunology: official organ of the International Association of Asthmology (INTERASMA) and Sociedad Latinoamericana de Alergia e Inmunología* 6 (3):208.
- Chuine, I., Belmonte, J., and Mignot, A. 2000. A modelling analysis of the genetic variation of phenology between tree populations. *Journal of Ecology* 88 (4):561-570.

-
- Cohen, M.B., Ecker, E., Breitbart, J., and Rudolph, J. 1930. The rate of absorption of ragweed pollen material from the nose. *The Journal of Immunology* 18 (6):419-425.
- Cohen, S.H., Yunginger, J.W., Rosenberg, N., and Fink, J.N. 1979. Acute allergic reaction after composite pollen ingestion. *Journal of Allergy and Clinical Immunology* 64 (4):270-274.
- Damialis, A., Gioulekas, D., Lazopoulou, C., Balafoutis, C., and Vokou, D. 2005. Transport of airborne pollen into the city of Thessaloniki: the effects of wind direction, speed and persistence. *Int J Biometeorol* 49 (3):139-145.
- ERDTMAN, G. 1986. *Pollen morphology and plant taxonomy: angiosperms*. Vol. 1: Brill Archive.
- ESRI, A. 2013. ArcGIS. Available from <http://www.esri.com/software/arcgis>.
- Fogh, C.L., and Andersson, K.G. 2000. Modelling of skin exposure from distributed sources. *Annals of Occupational Hygiene* 44 (7):529-532.
- Hansen, J.T., Koeppen, B.M., and Netter, F.F.H. 2002. *Netter's Atlas of Human Physiology*: Icon Learning Systems.
- Helbig, N., Vogel, B., Vogel, H., and Fiedler, F. 2004. Numerical modelling of pollen dispersion on the regional scale. *Aerobiologia* 20 (1):3-19.
- Hu, X., Zhang, Y., Luo, J., Wang, T., Lian, H., and Ding, Z. 2011. Bioaccessibility and health risk of arsenic, mercury and other metals in urban street dusts from a mega-city, Nanjing, China. *Environmental Pollution* 159 (5):1215-1221.
- Karl, T., and Koss, W.J. 1984. *Regional and National Monthly, Seasonal, and Annual Temperature Weighted by Area, 1895-1983*: National Climatic Data Center.
- Kartesz, J.T. 2013. The Biota of North America Program (BONAP), Taxonomic Data Center [maps generated from Kartesz, J.T. 2013. Floristic Synthesis of North

-
- America, Version 1.0. Biota of North America Program (BONAP). (in press)].
Chapel Hill, N.C. Available from <http://www.bonap.net/tdc>.
- Lamb, C.E., Ratner, P.H., Johnson, C.E., Ambegaonkar, A.J., Joshi, A.V., Day, D., Sampson, N., and Eng, B. 2006. Economic impact of workplace productivity losses due to allergic rhinitis compared with select medical conditions in the United States from an employer perspective. *Current Medical Research and Opinion*® 22 (6):1203-1210.
- Lu, W., and Howarth, A.T. 1996. Numerical analysis of indoor aerosol particle deposition and distribution in two-zone ventilation system. *Building and Environment* 31 (1):41-50.
- Saltelli, A., Chan, K., and Scott, E.M. 2000a. *Sensitivity analysis*. Vol. 134: Wiley New York.
- Saltelli, A., Tarantola, S., and Campolongo, F. 2000b. Sensitivity analysis as an ingredient of modeling. *Statistical Science* 15(4):377-395.
- Seinfeld, J.H., and Pandis, S.N. 2012. *Atmospheric chemistry and physics: from air pollution to climate change*: John Wiley & Sons.
- Shea, K.M., Truckner, R.T., Weber, R.W., and Peden, D.B. 2008. Climate change and allergic disease. *Journal of Allergy and Clinical Immunology* 122 (3):443-453.
- Singh, K., Axelrod, S., and Bielory, L. 2010. The epidemiology of ocular and nasal allergy in the United States, 1988-1994. *Journal of Allergy and Clinical Immunology* 126 (4):778-783. e6.
- Sofiev, M., Belmonte, J., Gehrig, R., Izquierdo, R., Smith, M., Dahl, Å., and Siljamo, P. 2013. Airborne Pollen Transport. In *Allergenic Pollen*: Springer.
- U.S Census Bureau. 2010. Profile of General Population and Housing Characteristics: 2010 Available from

http://factfinder2.census.gov/faces/tableservices/jsf/pages/productview.xhtml?pid=DEC_10_113_113DP1&prodType=table.

U.S. Census Bureau. 2010. Profile of General Population and Housing Characteristics: 2010

USEPA. 2010. Exposure factors handbook. US Environmental Protection Agency. Washington, DC. Available from <http://www.epa.gov/ncea/efh/pdfs/efh-complete.pdf>.

Zhang, Y., Bielory, L., and Georgopoulos, P.G. 2013a. Climate change effect on Betula (birch) and Quercus (oak) pollen seasons in the United States. *Int J Biometeorol*.

Zhang, Y., Isukapalli, S., Georgopoulos, P., and Weisel, C. 2013b. Modeling Flight Attendants' Exposures to Pesticide in Disinfected Aircraft Cabins. *Environmental Science & Technology* 47 (24):14275-14281.